5-31-2020

Sea Surface Microplastics: an Inshore-Offshore Gradient Off the Olympic Peninsula

Rosemary Wood
Portland State University

Sea Surface Microplastics: an Inshore-Offshore Gradient off the Olympic Peninsula

Authored By
Rosemary Wood

Portland State University
June, 2020

An undergraduate honors thesis submitted in partial fulfillment of the requirements for the degree of
Bachelor of Science in **University Honors** and
Environmental Science and Management
with a
Minor in Sustainability

Thesis Advisor
Elise Granek
PhD in Zoology (Marine Ecology focus)

Table of Contents

Abstract

The lack of baseline data regarding plastic debris moving through and accumulating in various environmental compartments creates a vast gap in the literature for a number of reasons. These include a current lack of codified methodology to characterize microplastics both in morphology and polymer type, as well as gaps regarding contamination control & validation techniques. In September of 2019, sea surface sampling was collected off the Olympic Peninsula, WA with the goal of addressing the following three research questions. First, is variability in microplastic abundance driven by transect location, distance from shore, both or neither? Second, how does microplastic type, in morphology and polymer composition, vary relative to transect location and distance from shore? Third, which environmental variables contribute to the patterns of microplastic variability in abundance and type? The project is to provide a distribution-abundance baseline for sea surface microplastics (2-3m deep) along two transects: La Push & Grays Harbor in Washington, USA. Organic matter digestion was performed using a KOH solution & incubation procedure. After measuring, photographing, and counting microplastics via a dissection microscope, lipophilic Nile Red dye (10µg/mL) was applied, and the MPs were fluoresced at 455nm wavelength & counted under the microscope again. We use the following metrics to count & characterize the MPs found: size (MP>63um), color, morphology (fragment, film, fiber, fiber bundle, foam, microbead, other), and plastic polymer type via micro-FTIR analysis. Microplastics count and type, independent environmental conditions, and geospatial location data will be analyzed using a t-test to compare transects. Multiple regression will be used to identify relationships to environmental variables and an NMDS ordination to compare dissimilarity within the multivariate characterization data.

Introduction

As plastic materials have become an embedded part of our societal function, their lifecycle through production, use, waste, and degradation has become a pertinent research topic aiming to describe the long-term impacts of our current anthropogenic system on ecosystems. The ubiquitous use of plastic materials forming synthetic textiles, personal care products, tires, paints & equipment has led to the exposure of parent materials to destruction, degradation & release into our waste systems as well as the environment at large.[1] While plastic pollution does consist of whole, mismanaged waste items – it also includes very small microplastics (MP: 5mm-1µm)[2] and nanoplastics (NP<1µm)[3]. Primary microplastics are defined by the International Union for Conservation of Nature (IUCN) as those "directly released into the environment as small plastic particles (<5mm size)" manufactured and released within those size categories, such as microbeads manufactured for personal care products. These primary MPs

[1] Boucher & Friot, 2017; Wu et.al. 2018; Worm et.al. 2017; Ryan et.al. 2015
[2] Shim et al., 2017; Granek et al., 2020; Boucher & Friot, 2017; Frias et al., 2019; Isobe et al., 2014; Prata et al., 2019
[3] Crawford & Quinn, 2017; Granek et al., 2020; Shim et al., 2017; Worm et.al. 2017

can eventually degrade into secondary microplastics themselves.[4] IUCN reported in 2017 that primary MPs are the origin & "globally responsible for…between 15 and 31% of all of the plastic in the oceans" – describing a significantly prevalent and pervasive pollutant worldwide. The authors go on to say the "global release of primary microplastics into the ocean was estimated at 1.5 million tons per year" varying between "0.8 and 2.5 Mtons/year" depending on an optimistic or pessimistic model.[5] Secondary microplastics are shed through the weathering & degradation of larger plastics into smaller pieces via mechanical, biological or photo-oxidative means – including microfibers from fleece, fragments of marine paint or tire dust.[6].

Largely unseen by the naked eye, this novel form of pollution has potentially profound effects on our ecological systems; particularly at the estimated volumes of release. However, this research is complicated by a lack of codified methodology & the associated difficulties encountered when trying to account for representative sample sizes, contamination vectors, nondestructive MP extraction techniques, and a standardized system of morphological characterization.[7] Coupling this methodological struggle with the novel & extreme scope of anthropogenic debris release into the environment caused a paradigm shift in the discourse away from the question of their definition & presence towards a focus on characterizing the types & proportions of MPs in different ecosystem compartments along with their sources.[8] Our recognition of microplastics as a novel, emerging pollutant was kindled by detecting high densities of MP in beach sands, then made urgent by the discovery of the North Pacific Garbage Patch[9] – at which point the focus began to address the physical mobility of MPs through the connectivity of terrestrial, riverine & marine systems.[10] Extensions of this research could include identifying the roles of wastewater treatment plant systems (WWTP) and other urban gradient factors in releasing & transporting MPs while tracking their abundance and distribution into marine systems.[11] In doing so, the chemical type of plastic began being used to characterize potential sources of these MPs – matching them to things like tire or paint dust, household personal care products or commercial activities.[12] These are important, catalogued baselines that inform global distributions from transects at sea.[13] While much of the discourse is dedicated to marine abundance/distribution & waste water in stream systems, there has been recent recognition of wind pathways as well as road runoff as potentially significant sources.[14]

As the pervasive nature of anthropogenic MP release has become clear, characterizing their chemical and morphological nature shed light on the ways their presence changes biotic and abiotic systems. Exploring the effects of MPs on aquatic ecosystem compartments & the complex series of MP morphologies and chemical types that an ecosystem is exposed to may describe drivers in variability of ecosystem response. Microplastics with different morphological/polymer characteristics are able to absorb and transport toxins from their surroundings in different proportions - leaching them into the ecosystem compartments they accumulate – like sediments, aquatic surfaces & biota.[15] Some MPs float at water surfaces while others sink onto sediments or are taken up by biota based on their inherent physical or chemical characteristics. This uptake into biological systems provides a vector for bioaccumulation in two ways – physical build up of MPs or bioaccumulation of chemical pollutants sorbed/leached by the ingested MPs.[16] Worm's 2017 study found that "many plastics have the capacity to absorb both organic

[4] Masura et.al. 2015; Brandon, 2017; Boucher & Friot, 2017; Worm et.al. 2017; Goldstein et.al. 2013
[5] Boucher & Friot, 2017
[6] Boucher & Friot, 2017
[7] Masura et.al. 2015; Michida et.al. 2019; Hu et.al. 2019; Boucher & Friot, 2017; Henry et.al 2019
[8] Law, 2017; Ryan, 2015; Worm et.al. 2017
[9] Moore et.al. 2001; Goldstein et.al. 2013; Desforges et.al. 2014; Mendoza & Jones, 2015
[10] Ryan, 2015; Sun et.al. 2019; Li et.al. 2018; Leslie et.al. 2017; Hu et.al. 2019; Boucher & Friot, 2017; Law, 2017
[11] Granek et.al. 2016; Leslie et.al. 2017; McCormick et.al. 2014; Profita & Burns, 2019; Rodrigues et.al. 2018; Windsor et.al. 2019
[12] Boucher & Friot, 2017; Falco et.al.2019
[13] Boucher & Friot, 2017; Li et.al. 2018; Carr et.al. 2016; Law, 2017; Raju et.al. 2018; Mason et.al. 2016
[14] Cincinelli et.al. 2017; Desforges et.al. 2014; Di Mauro, 2017; Gorokhova, 2015; Henry et.al. 2019; Hidalgo-Ruz et.al. 2012; Hu et.al. 2019; Isobe et.al. 2014; Li et.al. 2018; Worm et.al. 2017; Boucher & Friot, 2017
[15] Anbumani & Kakkar, 2018; Brandon, 2017; Windsor et.al. 2019; OR&R Marine Debris Division, 2015; Wardrop et.al.2016; Raju et.al. 2018; Mendoza & Jones, 2015; Shim et.al 2017; Kedzierski et.al. 2019
[16] Brandon, 2017; Mendoza & Jones, 2015; Hu et.al. 2019; Wardrop et.al. 2016; Raju et.al. 2018

and metal pollutants from the environment and concentrate [them] up to 1 million-fold relative to concentrations found in seawater" indicating a growing impact the longer the issue is avoided.[17] Based on current studies regarding MP uptake by plankton[18], filter feeders[19] & macroinvertebrates[20] – the increased bioavailability of microplastics as microbial biofilm substrate[21] (resulting in unique community assemblages) & trophic bioaccumulation[22] of both physical MPs and their sorbed chemicals may impact not only the overall ecosystem function but also human health. Biological-MP impacts have been found across scales - from altered gene expression, cellular division & fatty acid metabolism at the sub/cellular level to altered feeding & reallocation of energy reserves in individual organisms leading to reduced growth, reproductive output and offspring viability of populations.[23]

Scientific research has articulated the presence of inshore-offshore gradient patterns in a number of marine conditions, including but not limited to: phytoplankton distribution[24], temperature,[25] dissolved oxygen[26] and nutrients.[27] However, microplastics have not yet been fully assessed for this pattern as an emerging contaminant. To better characterize patterns in sea surface microplastics off the coast of the Olympic Peninsula and identify potential drivers of those patterns the following research questions and hypotheses were examined:

1. ***Is variability in microplastic abundance driven by transect location, distance from shore, or both?***
    a. **H_1:** Variability in microplastic abundance will be more significantly driven by distance from shore than by transect location, though both will have an influence.
    b. **H_2:** Variability in microplastic abundance will be more significantly driven by transect location than distance from shore, though both will have an influence.
2. ***How does microplastic type, both in morphology and polymer composition, vary relative to transect location and distance from shore?***
    a. **H_1:** Microplastic morphology will vary more significantly than polymer composition relative to distance from shore - with microfibers being found in greater abundance than any other morphology.
    b. **H_2:** There will be a positive trend in abundance of the following polymer types of microplastics inshore: those more closely associated with terrestrial sources (*e.g.*, tire dust) as well as higher density polymers that may not keep buoyancy offshore. There will be a greater abundance of microfibers and low density polymers offshore.
3. ***Which environmental variables contribute to the patterns in microplastic abundance and type across transects?***
    a. **H_1:** There will be a greater total abundance of microplastics inshore compared to offshore due to the seasonality of late September sampling - as seasonal shifts in large scale surface wind patterns favor inshore movement during the sampling season.

Hypotheses were determined using the available literature and data regarding the fall of 2019 & historic seasonal patterns in downwelling/upwelling off the Olympic Peninsula (which causes inshore/offshore sea surface movement, respectively).[28] This, combined with the potential influence of

[17] Worm et.al. 2017
[18] Brandon, 2017; Law, 2017; McCormick et al. 2014
[19] Baechler et.al. 2019; Dehaut et.al 2016; Di Mauro, 2017; Gorokhova, 2015; Granek et.al. 2016; Piarulli et.al. 2019
[20] Leslie et.al. 2017; Scherer et.al. 2017; Windsor et.al. 2019
[21] Hu et.al. 2019; Michielssen et.al. 2016; Worm et.al. 2017; Kettner et.al 2019; McCormick et.al. 2014
[22] Baechler et.al. 2019; Henry et.al. 2019; Wardrop et.al. 2016; Pershing et.al. 2015
[23] Worm et.al. 2017
[24] Northwest Fisheries Science Center, 2018
[25] Puget Sound Institute, 2007; NOAA: National Centers for Environmental Information (formerly the National Climatic Data Center), 2020
[26] Northwest Fisheries Science Center, 2019
[27] Northwest Fisheries Science Center, 2019
[28] Puget Sound Institute, 2007

the southeast expansion of the Aleutian Low on sea surface, contributes to "onshore flow into the Pacific Northwest from October through early spring".[29]

Methodology

I ▸ *Study Site*

Sampling took place along two transects off the Olympic Peninsula, Washington – at Grays Harbor (47.1°N) & La Push (47.92°N), each consisting of 7 stations sampled along latitudinal constants ***(Fig.1)***. The subsequent lab processing & analyses took place in Portland State University's Applied Coastal Ecology lab and validation was supported by micro-FTIR analysis in collaboration with the Brander lab at Oregon State University.

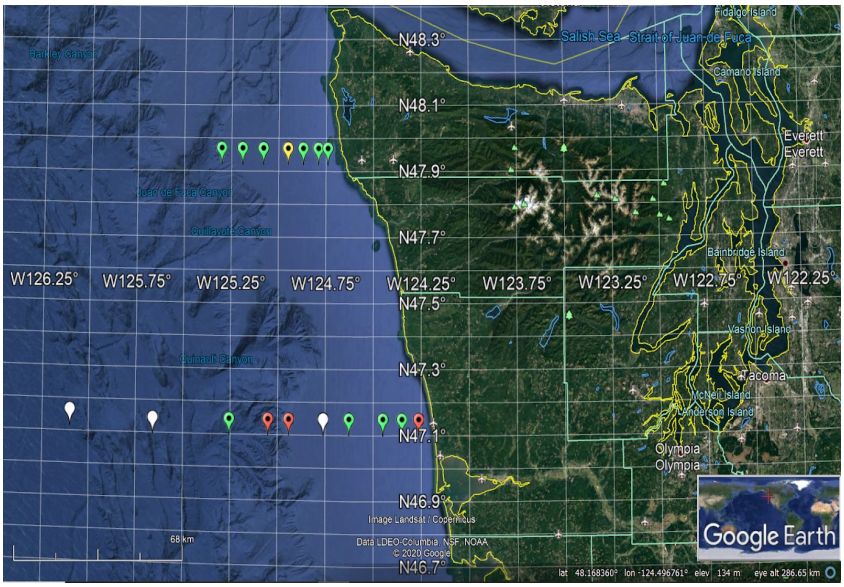

Fig.1 - Transect Map

Map of field sampling regime along two transects (top: La Push; bottom: Grays Harbor) off the coast of the Olympic Peninsula. Each pin corresponds to a sampling station, and the color corresponds to the number of subsamples obtained on site (green: 3; yellow: 2; red: 1; white: no data able to be collected due to weather conditions or lack of time on station).

II ▸ *Field Sampling*

Sites selected were accessible via the long term monitoring efforts of the NOAA research vessel *Bell M. Shimada*, conducted over September 19th-29th, 2019. Grays Harbor (47.1°N) & La Push (47.92°N) have no baseline data for sea surface microplastics & will contribute significant data to contextualize Pacific NW contaminant data-basing efforts ***(Table.1)***. Sampling regimes were adjusted based on OSU Master's student Anna Bolm's sea surface sampling methodology using the shipboard seawater intake system from about 2-3 meters below the surface using a vacuum pump.[30]

Table.1 - Sampling stations' Latitude & Longitude

Table of station latitude & longitude by transect (lower station numbers are closer to shore). Colors of each station ID correspond to the number of subsamples obtained on site (green: 3; yellow: 2; red: 1).

La Push	LP04	LP06	LP09	LP12	LP17	LP22	LP27

[29] Puget Sound Institute, 2007

[30] A. Bolm & R. Wood, personal communication, 2019; Shim et al., 2017; Prata et al., 2019

(Lat; Long)	47.92; -124.74	47.92; -124.79	47.92; -124.87	47.92; -124.95	47.92; -125.08	47.92; -125.19	47.92; -125.30
Grays Harbor	**GH01b**	**GH02b**	**GH04b**	**GH05b**	**GH08b**	**GH09b**	**GH45b**
(Lat; Long)	47.10; -124.264	47.10; -124.351	47.10; -124.45	47.10; -124.6262	47.10; -124.94	47.10; -125.0477	47.10; -125.25

At each station, three subsamples were taken, unless weather or timing made that impossible (as was the case for the following stations: LP12; GH01b; GH08b; GH09b). The shipboard water intake was fitted with a flow meter & the sample volume (~50L) was run through a covered sieve tower with mesh sizes: 250µm, 120µm, and 63µm. Each of those sieves was then rinsed three times using filtered sea water (FSW) into a vacuum pump system fitted with a 0.7µm borosilicate glass microfiber filter (GF/F; WHA1825047).[31] The vacuum pump system was covered with an aluminum foil cap during filtration to avoid contamination & the flow time was recorded, aiming for 15 minutes but cutting to 10 minutes if the itinerary didn't allow more time on station. Once the vacuum pumping was finished, the filter was folded in half (to protect collected microplastics), wrapped in aluminum foil, labeled and frozen at -12 °C ***(Fig.2)***.

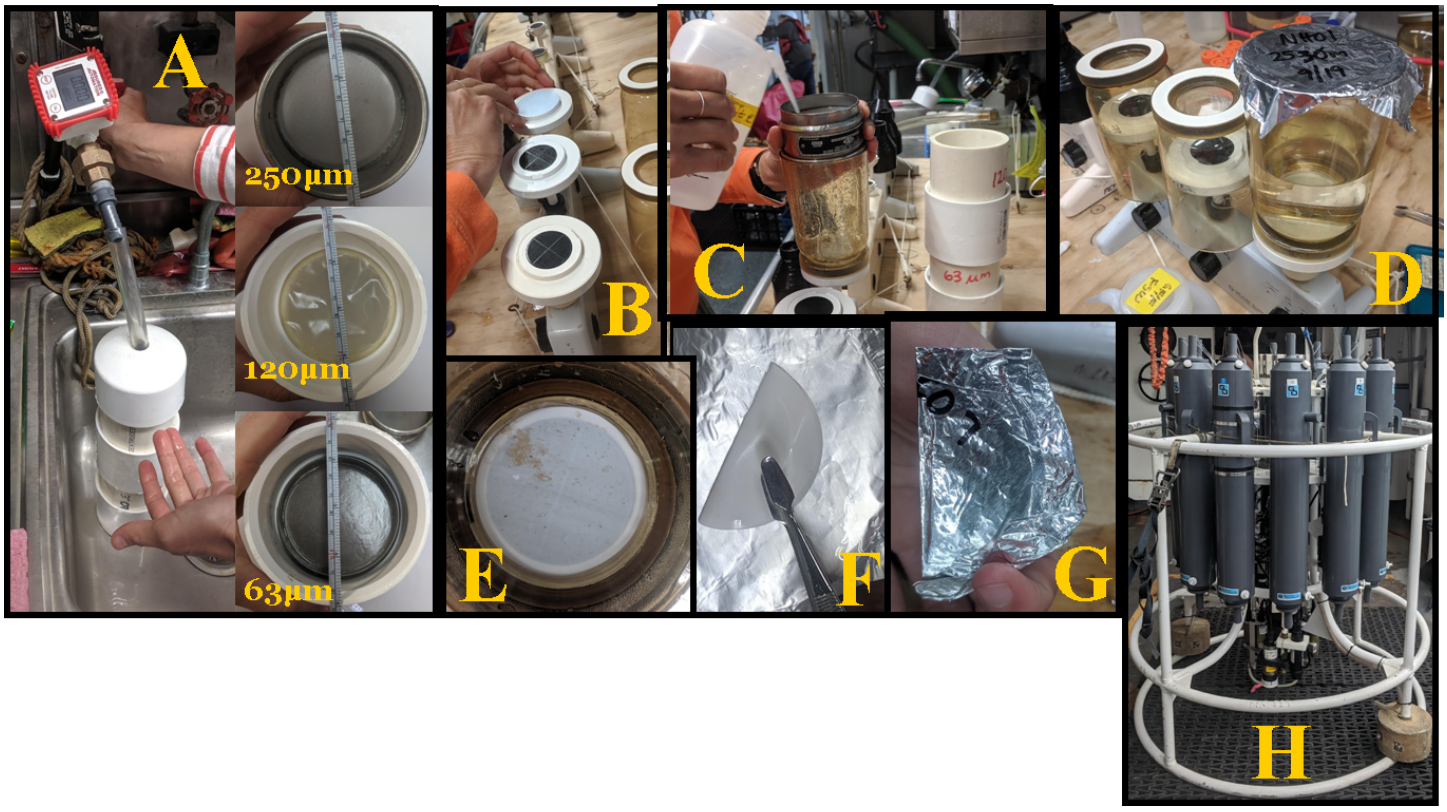

Fig.2 - Field Sampling Method

A) *Shipboard sea water intake from ~2-3m depth with flow meter on intake & Sieve Tower in sink - (Mesh sizes = top: 250µm, middle: 120µm, bottom: 63µm);* ***B)*** *0.7µm pore size GF/F glass microfiber filter placement on vacuum pump rig using forceps;* ***C)*** *Rinse all 3 sieves, 3x onto 1 filter on vacuum pump using FSW;* ***D)*** *Cover pump with aluminum foil to decrease aerial contamination;* ***E)*** *Fully filtered sample before removal from vacuum rig;* ***F)*** *Remove filter using forceps, fold in half;* ***G)*** *Wrap in aluminum foil & freeze at -12℃;* ***H)*** *CTD Rosette and ships instruments report independent variables*

[31] Carr, Liu, & Tesoro, 2016; Cincinelli et al., 2017; Cole et al., 2014; EMD Millipore Corp., 2015; Falco, Pace, Cocca, & Avella, 2019; Leslie, Brandsma, van Velzen, & Vethaak, 2017; Thermo Fisher Scientific Inc., 2014; Valine, 2019; Thermo Fisher Scientific, 2014

Independent variables were gathered via the ship's instruments & the CTD Rosette attached to Niskin bottles used for generalized NOAA monitoring at depth. The independent variables collected include:

- Station GPS location (SciGPS-Lat; SciGPS-Lon)
- Ship Speed (SciGPS-SOG: "Speed Over Ground")
- Date (mm/dd/yyyy) & Time (hh:mm)
- Sea Surface Temperature (°C)
- Conductivity (S/m)
- Salinity (practical salinity unit; g/kg)
- Dissolved Oxygen (ppm)
- Chlorophyll max depth via fluorescence (mg/m^3)
- Nutrients at discrete depths
- Depth at station (m)
- Air Temperature (°C)
- Wind Speed (knots) & Direction (degrees)
- Relative Humidity
- Air Pressure (hPa)

To minimize contamination, each sampler (R. Wood, A. Bolm) wore a 100% cotton, orange sweatshirt, providing a metric for analysis to control for orange fibers as sample contamination during field collection. Filtered sea water (FSW) for processing and controls was collected either: via the shipboard intake, filtered through clean GF/F 0.7µm pore filter and stored or reclaimed from the vacuum pump system as sample sieves were rinsed into the pump system during normal processing through sample GF/F 0.7µm pore filters & stored for use. The sample controls consisted of two types: an Environmental Control (EC) and a Procedural Control (PC), one for each transect. Environmental controls (EC) took the form of a clean filter, wetted with FSW and exposed to the air while sampling was taking place for each transect & covered between samples. Procedural controls (PC) took the form of the same sampling methodology from sieving to storage undertaken using ~20L FSW to replace sample water from the seawater intake - accounting for any contamination via the equipment[32] ***(Fig.3)***.

Fig.3 - Environmental Control & Procedural Control
A) *Orange, 100% cotton sweatshirt worn during field sampling;* ***B)*** *Environmental Control (EC) filter next to field sample filtering station;* ***C)*** *Sea water filtered through a vacuum pump & 0.7µm GF/F filter, after which ~20L were collected in the carboy, then poured over the sieve towers and processed through the vacuum pump onto a filter like a field sample*

III ▸ *Lab Processing*

0 ◆ *Trial Run*

The overarching goals of the Trial Run Treatments were to identify the best methodological approach for digestion of organic matter on pre-filtered field samples without compromising the integrity of the collected sea surface microplastics (MP) - avoiding damage, loss or degradation during

[32] A. Bolm & R. Wood, personal communication, 2019

processing.[33] To do so, the efficiency of the potassium hydroxide (KOH) digestion method was qualitatively determined and the ability to visually identify MPs via microscope among the borosilicate glass microfibers of the filter itself was confirmed. Alternatives such as acidic removal[34] and wet peroxide oxidation (WPO)[35] were avoided due to degradation potential, and safer options such as enzyme digestions[36] were avoided due to cost and the contamination vulnerability due to their multi-stepped process. The Trial Run consisted of 3 treatments to address five key troubleshooting questions summarized in the table below ***(Table.2)***. Each treatment was applied to the same eight filters in a matrix as they moved through the processing stages associated with each Trial Run Treatment - Treatment 1 relates to field sampling collection & storage; Treatment 2 pulls apart the variables affecting KOH digestion efficiency; and Treatment 3 outlines the optimal setting for visual identification via microscope while minimizing MP loss due to increased mobility ***(Table.2, Fig.5)***. This process was key to maintain confidence in the processing of our field samples and coalescing a nondestructive method for pre-filtered samples that has been overshadowed in the literature due to the majority of studies using some form of free-floating samples (water, tissue or sediment) & a density-separation protocol to isolate MPs - either before or during organic matter digestion. Those methods must be adjusted to accommodate filter samples that need to have the organic matter digested away in order to identify MPs. During the planning process the Whatman GF/F 0.7µm borosilicate glass microfiber filter (WHA1825047; Sigma Aldrich) was selected for its' inert nature regarding numerous organic matter digestion methods, as opposed to using Mixed Cellulose Ester filters (0.45µm pore size)[37] as these filters are vulnerable to breaking down under digestion conditions, potentially contributing to difficulty in microscope visual identification.[38]

The Trial Run was conducted on a total of eight GF/F filters, each filtered (using a vacuum pump) with a homogenized blend of 200mL local Willamette River water and 1mL organic matter collected from Portland, Oregon's East Bank in the first week of March, 2020 ***(Fig.4)***. After filtration, Treatment 1 was applied as four of the filters were labelled *"Whole"*, wrapped in aluminum foil as flat disks and stored, and frozen. The other four were labelled *"Folded"*, folded in half to mimic the field sample filter state, and then frozen. This allows for clarification on how difficult it is to differentiate between the broken glass microfibers that make up the filter and MPs (particularly transparent microfibers).[39] Treatment 2 yields three key points of methodological clarification based on the potassium hydroxide (KOH) organic matter digestion method fully articulated in the following section. First, identify the appropriate weight/volume dilution concentration of KOH *(5% or 10%)* in filtered DI water in order to apply 15mL using a pasteur pipette & effectively digest the majority of organic matter without degrading any present MPs. After determining the concentration, the best length of time left to digest at room temperature *(16-24 hrs)* must be identified, along with how long *(24-48 hrs)* is needed to completely dry the remaining 15mL of KOH solution in each dish when placed in the drying oven at 40°C. Treatment 3 identifies the necessary volume of filtered DI water with which to rehydrate the filter during visual microscope MP identification & characterization. With greater volumes *(5mL)*, the MPs may become dislodged from the filter and migrate more easily during counting, however, this may be overshadowed by the potential loss of MP if examined on a comparatively dry filter *(1mL)* - as the lack of surface tension could allow MPs to be sprung off the filter entirely during probe examination ***(Fig.5)***.

[33] EMD Millipore Corp., 2015; Baechler, 2019; B. Baechler, personal communication, January 9, 2020; Thiele et al., 2019; Dehaut et al., 2016; Prata et al., 2019; Piarulli et al., 2019; Herrera et al., 2018
[34] Prata et al., 2019; Cole et al., 2014; Herrera et al., 2018
[35] Mausra et al., 2015; Michida et al., 2019; Prata et al., 2019; Herrera et al., 2018
[36] Löder et al., 2017; Cole et al., 2014; Piarulli et al., 2019
[37] A. Bolm & R. Wood, personal communication, 2019
[38] B. Baechler, personal communication, January 9, 2020
[39] EMD Millipore Corp., 2015

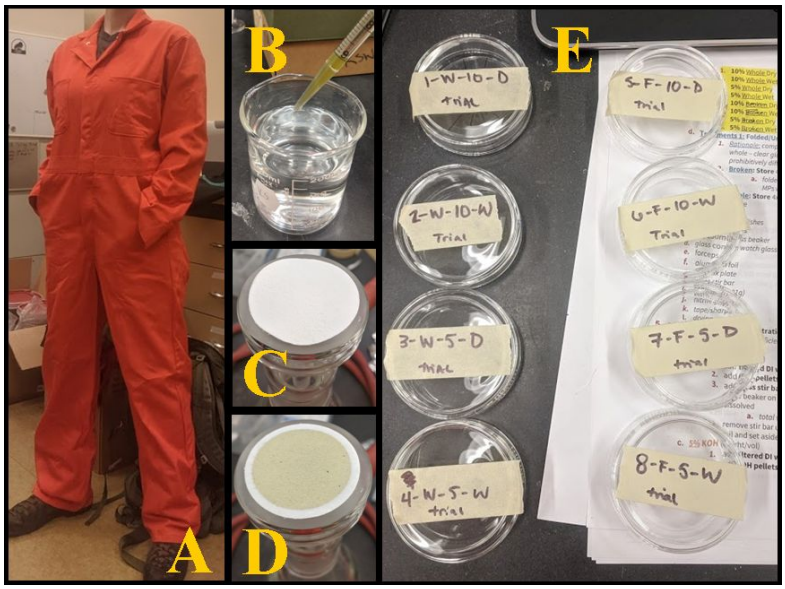

Fig.4 - Trial Run Filters

A) *Lab QA/QC: 100% cotton, orange lab coveralls worn during all lab processing;* ***B) Treatment 1:*** *200mL Willamette River water collected from East Bank, Portland, OR with 1mL of homogenized organic matter (goose feces from same collection site);* ***C) Treatment 1:*** *Clean GF/F Filter on the glass lab vacuum pump before filtration;* ***D) Treatment 1:*** *GF/F Trial Run filter after trial organic matter has been filtered through;* ***E)*** *labelling regime of trial run filters: (Petri.Dish#)-(T1: Whole/Folded)-(T2: KOH%)-(T3: Wet/Dry)*

Table.2 - Trial Run Treatment Regimes & Rationale

Treatment #	**Relevance/Need**	**Troubleshooting Questions**	**Treatment Structure & Rationale**	
T1: Folded/Whole	**Field Sample filters were folded in half, often breaking along the fold,** before being wrapped & frozen in storage	Can I ID MPs among broken glass filter microfiber textures due to the fold?	**Folded:** folded in half to mimic field samples, store frozen wrapped in foil	**Unfolded/Whole:** unfolded filters, store frozen & wrapped in foil
T2: Digestion Efficiency & Avoiding MP Degradation	**T2-A: Concentration KOH**	What concentration of KOH is appropriate for 15mL of solution to efficiently digest organic matter without degrading MPs?	**5%** w/v **KOH Solution** (1.292105 Molarity) (pH=14.1)	**10%** w/v **KOH Solution** (1.33996 M) (pH=14.1)
	T2-B: Digestion Time	How long is needed to efficiently digest organic matter in 15mL of (T1%) KOH solution without degrading MPs?	**16 hours** @ room temperature in fume hood	**24 hours** @ room temperature in fume hood
	T2-C: Drying Time	How long is needed to completely dry 15mL of (T1%) KOH solution in each sample filter petri dish?	**24 hours** @40°C in drying oven	**48 hours** @40°C in drying oven
T3: Visual Microscope MP ID	**Volume filtered DI water added** for ease of visual ID MPs	How does MP mobility on the filter during identification change depending on the volume of water added? What is the danger of rewetted KOH to the microscope during ID?	**Dry (1mL)** determine MP mobility on filter	**Wet (5mL)** determine MP mobility on filter

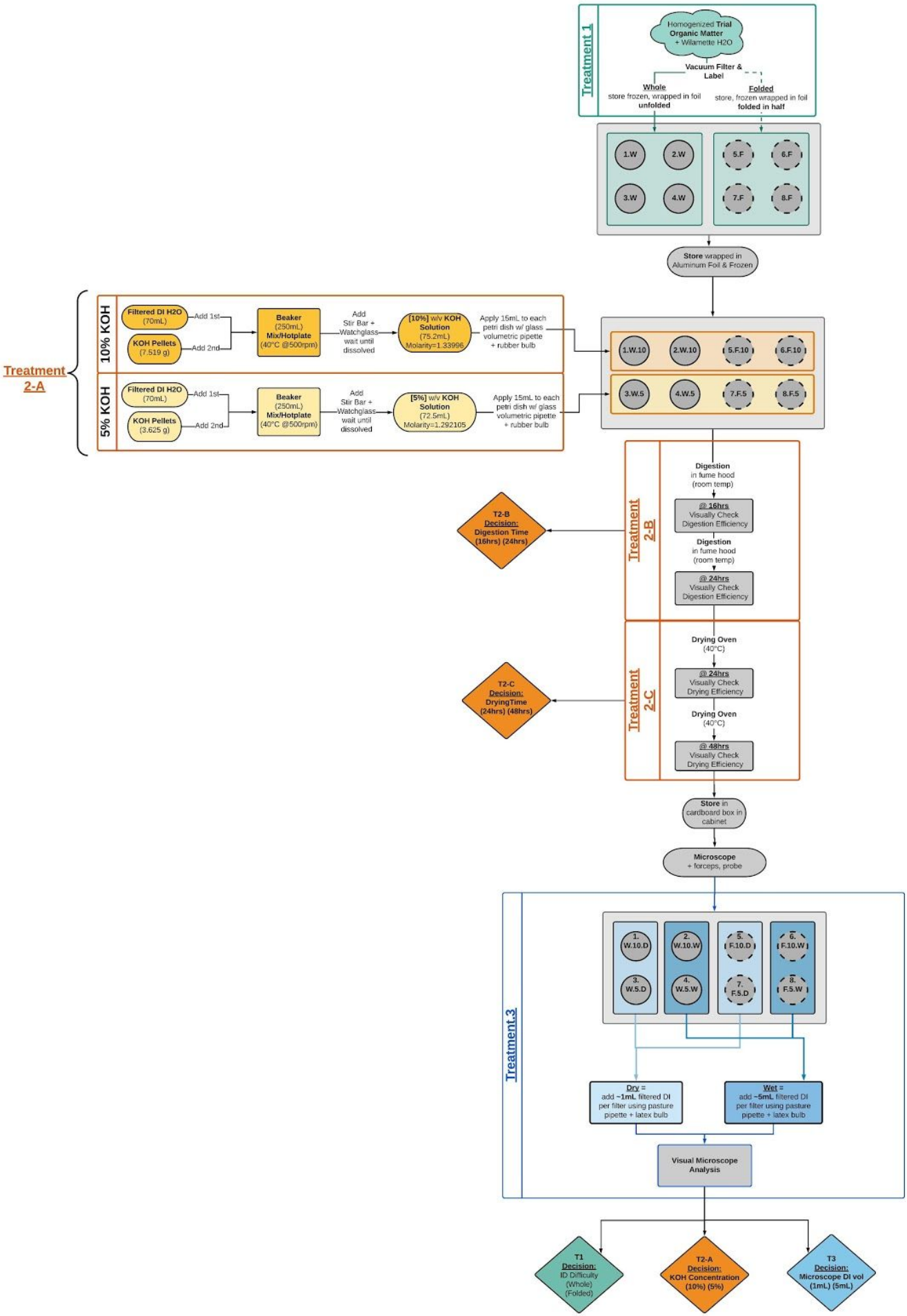
Treatment 1
Homogenized Trial Organic Matter + Willamette H2O
Vacuum Filter & Label
Whole
store frozen, wrapped in foil unfolded
Folded
store, frozen wrapped in foil folded in half
1.W
2.W
3.W
4.W
5.F
6.F
7.F
8.F
Store wrapped in Aluminum Foil & Frozen
Treatment 2-A
10% KOH
Filtered DI H2O (70mL)
Add 1st
KOH Pellets (7.519 g)
Add 2nd
Beaker (250mL) Mix/Hotplate (40°C @500rpm)
Add Stir Bar + Watchglass wait until dissolved
[10%] w/v KOH Solution (75.2mL) Molarity=1.33996
Apply 15mL to each petri dish w/ glass volumetric pipette + rubber bulb
5% KOH
Filtered DI H2O (70mL)
Add 1st
KOH Pellets (3.625 g)
Add 2nd
Beaker (250mL) Mix/Hotplate (40°C @500rpm)
Add Stir Bar + Watchglass wait until dissolved
[5%] w/v KOH Solution (72.5mL) Molarity=1.292105
Apply 15mL to each petri dish w/ glass volumetric pipette + rubber bulb
1.W.10
2.W.10
5.F.10
6.F.10
3.W.5
4.W.5
7.F.5
8.F.5
Treatment 2-B
Digestion in fume hood (room temp)
@ 16hrs Visually Check Digestion Efficiency
Digestion in fume hood (room temp)
@ 24hrs Visually Check Digestion Efficiency
T2-B Decision: Digestion Time (16hrs) (24hrs)
Treatment 2-C
Drying Oven (40°C)
@ 24hrs Visually Check Drying Efficiency
Drying Oven (40°C)
@ 48hrs Visually Check Drying Efficiency
T2-C Decision: DryingTime (24hrs) (48hrs)
Store in cardboard box in cabinet
Microscope + forceps, probe
Treatment 3
1. W.10.D
2. W.10.W
5. F.10.D
6. F.10.W
3. W.5.D
4. W.5.W
7. F.5.D
8. F.5.W
Dry = add ~1mL filtered DI per filter using pasture pipette + latex bulb
Wet = add ~5mL filtered DI per filter using pasture pipette + latex bulb
Visual Microscope Analysis
T1 Decision: ID Difficulty (Whole) (Folded)
T2-A Decision: KOH Concentration (10%) (5%)
T3 Decision: Microscope DI vol (1mL) (5mL)

Fig.5 - Concept Map: Trial Run Treatment Regime

This chronological flow chart (top to bottom) describes successive treatments to the same 8 filters throughout. These filters are represented by the gray circles (T1: solid=whole, dotted=folded) and with each step they are assigned label notation ("Filter ID#.T1.T2A.T3" within each circle). Diamonds represent decision points, color coded by treatment (see Table.2 for further descriptions of treatment rationale) which informs the final lab processing methods (Organic Matter Digestion; Microscope Visual Analysis).

1 ◆ *Organic Matter Digestion*

Potassium hydroxide (KOH)[40] was chosen as the most appropriate method of effective organic matter digestion based on the anticipated concentration & digestion time. KOH has the potential to degrade or destroy MPs over time or under high temperatures - as do other common methodologies: wet peroxide oxidation (WPO)[41] and enzyme digestion.[42] However, KOH was more accessible both financially & logistically than the other methods as enzyme digestion contains numerous opportunities for contamination due to its multi-stepped digestion, and WPO was more complex to apply to a prefiltered sample as opposed to free floating MP sample mixtures.[43]

All 39 field samples were randomized in excel and split into three batches of 13 (Batch A, B, C) due to time & space constraints for processing. Each batch was assigned a Digestion Control (DC) and a Nile Red Control (NRC) in excel. The filters in each batch were then assigned Sample ID Numbers (A=#1-15; B=#16-30; C=#31-45), after which a 60mm glass covered petri dish was labelled and prepared with a pie-cut petri dish sticker (12 sector) for each filter - including DC & NRC ***(Fig.6)***.

The appropriate concentration of KOH was prepared according to the result of Trial Run Treatment 2-A (10% or 5%) in a weight-by-volume solution of KOH pellets dissolved with a stir bar in 250mL (per batch) of 40°C DI water on a 500rpm stir plate while covered with a concave watch glass. Once the KOH digestion solution was fully dissolved, the batch of filters being processed and their associated petri dishes were moved to the fume hood. The NRC petri dish was set aside for this processing step. First, the DC petri dish was opened, a clean new filter was placed in it, after which it was wetted with 5mL of DI water. The DC dish was left open to the fume hood to quantify potential aerial contamination for the remainder of the batch. Each field sample was individually opened from the foil, its associated petri dish opened, the filter transferred using forceps, and 15mL of the KOH digestion solution was gently added using a glass volumetric pipette & rubber bulb. Each dish was closed before moving on to the next, but once the field samples were complete the DC dish then had 15mL of the KOH solution gently added in the same manner as the others. The batch was then left to digest in the fume hood at room temperature for the number of hours determined by Trial Run Treatment 2-B (16hrs or 24hrs) before being dried at 40°C in the drying oven for the number of hours determined by Trial Run Treatment 2-C (24hrs or 48hrs). All the digested batches were stored - taped closed- in a cardboard box in a dark cabinet ***(Fig.6)***.

[40] EMD Millipore Corp., 2015; Baechler, 2019; Thiele et al., 2019; Dehaut et al., 2016; Prata et al., 2019; Piarulli et al., 2019; Herrera et al., 2018; Lusher et al. 2017

[41] Mausra et al., 2015; Michida et al., 2019; Prata et al., 2019; Herrera et al., 2018; Lusher et al. 2017

[42] Löder et al., 2017; Cole et al., 2014; Piarulli et al., 2019; Lusher et al. 2017

[43] Baechler, 2019; Mausra et al., 2015

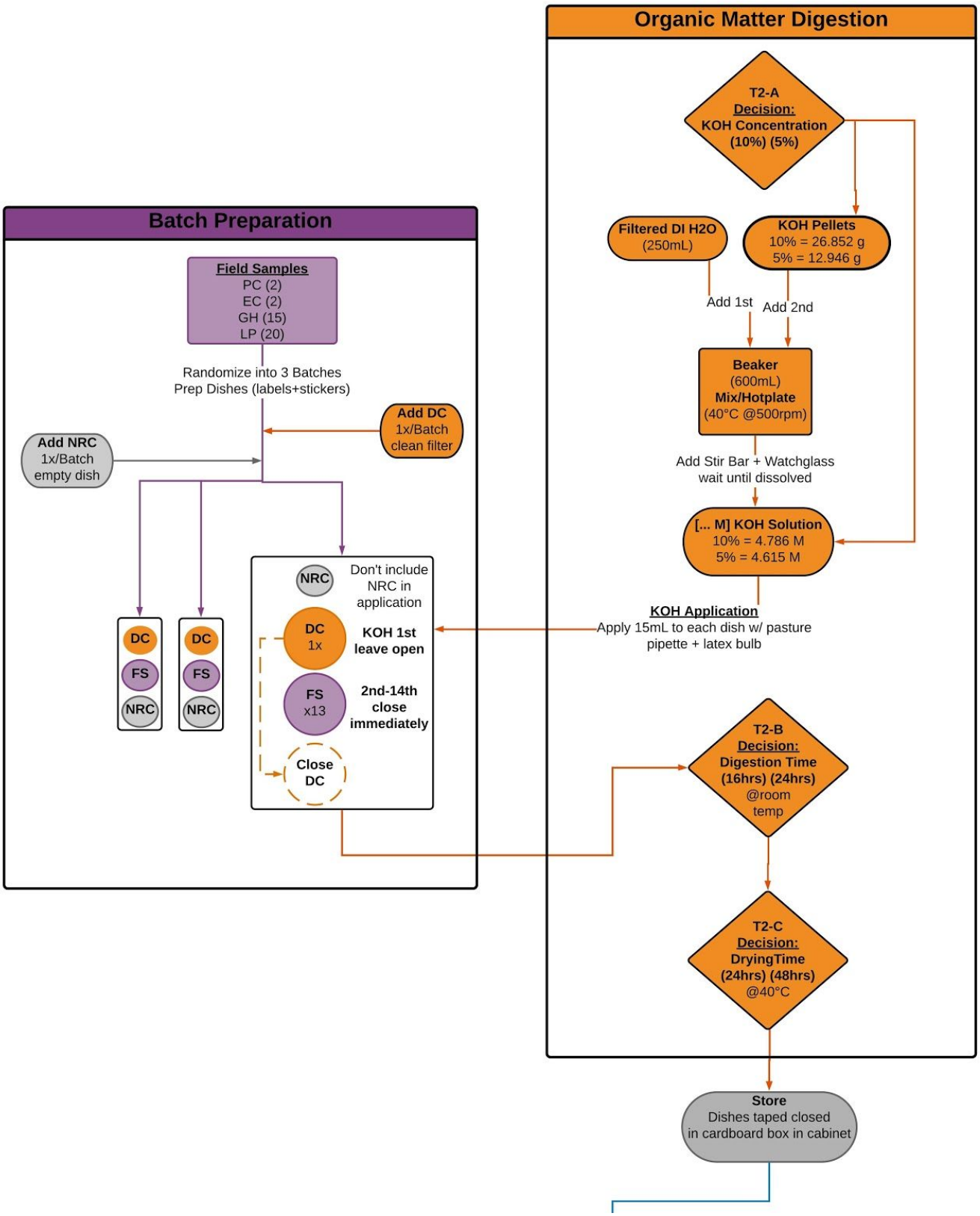

Fig.6 - Concept Map: Sample Preparation & Organic Matter Digestion

A chronological flow chart describing the lab processes involved in the preparation of samples and digestion of organic matter in potassium hydroxide. The left swim lane contains the steps involved in sample batch preparation (purple = field samples) including the addition of one Digestion Control per batch (DC=orange) utilized in this step, as well as one NRC per batch which is utilized later in lab processing. The right swim lane contains the process the batches each go through in order to digest (orange). The diamonds represent decision information from the results of relevant Trial Run Treatments.

2 ◆ *Pre-Nile Red Microscope Visual Analysis*

To prepare the Leica Dissecting Microscope area for visual analysis of MP samples, a snorkel fume hood was put in place to minimize aerial contamination during processing. A covered 100mL beaker containing ~20mL DI water, a very fine probe, forceps and a glass pasteur pipette were gathered to assist manipulating MPs.[44] The visual assessment involved identification of MPs, characterization of their morphology, and photography of identified samples.[45] Potential MPs were assessed using the following selection criteria (best for the size range 0.5-5mm) & standardised Size and Colour Sorting (SCS) system from Crawford & Quinn (2017)[46] with adjustments to reflect the structure of control regimes and the lower limit of our GF/F filter catchment capacity (0.7µm pore size) ***(Table.3)***.

Selection Criteria[47]

- *The particle or fibre in question has no observable organic or cellular structures.*
- *Particles should be uniformly colored.*
    - *In the case of transparent, opaque or white particles, further high-magnification microscopic examination, as well as fluorescence microscopy, should be undertaken to preclude the possibility of biological origin*
- *In the case of fibres, the diameter should be consistent along the length with no evidence of tapering or bending in three-dimensional space. If the fibre is not straight, biological origin is suspected.*
    - *In the case of red coloured fibres, additional scrutinisation with high-magnification microscopic examination, fluorescence microscopy and staining of chloroplasts is required to preclude algal sprouts.*

Identification was determined using precision forceps and the fine probe to test the potential MP for malleability and breakage - and rolled using the probe to compare to glass or sand texture.[48] Using the petri dish sticker as a guide, each microplastic was identified and assigned an MP ID label constructed of the following data: *(Filter ID#)-(Sector of Filter)-(cumulative # MP found on filter)-(Morphology.Code)-(Color.Code).* As an example, if a microplastic photograph was labeled as the following *(15)-(4)-(12)-(MFB)-(LT.PR)* it would be interpreted as *a light purple microfiber (12th of total MP found on filter #15, sector 4)* and its size would be in the associated data sheet. Each MP was measured and photographed using Leica Microscope software. Each photograph was named according to the MP ID label structure.

Table.3 - Characterization: Morphology & Color Categories

Summary tables adapted from Crawford & Quinn, 2017 of ***A)*** *Morphological/size categories as well as* ***B)*** *Color codes - used to identify and categorize based on MP identification methodology outlined above. Both the Morphology codes (top, grey) and the Color codes (bottom, grey & yellow) were used throughout the Pre-NR microscope analysis, but during the Post-NR microscope analysis only the Morphology code was recorded as the fluorescence of MPs dyed with Nile Red circumvented the need for MP pigment notation at this step. However, after the Post-NR analysis the second count of NRC (NRC2) was also assessed under normal light conditions and Color codes were recorded to assess potential aerial contamination during Post-NR microscope analysis.*

[44] B. Baechler, personal communication, January 9, 2020
[45] Baechler, Granek, et al., 2019; Baechler, Stienbarger, et al., 2019; (Boucher & Friot, 2017; Brandon, 2017; Dehaut et al., 2016; Desforges et al., 2014; Di Mauro, 2017; Falco et al., 2019; Frias et al., 2019; Hidalgo-Ruz et al., 2012; Li et al., 2018; Mausra et al., 2015; Mendoza & Jones, 2015; Michida et al., 2019; Moore et al., 2001; Prata et al., 2019; Shim et al., 2017
[46] Crawford & Quinn, 2017 (pg.220-232)
[47] Crawford & Quinn, 2017 (pg.220-232)
[48] B. Baechler, personal communication, January 9, 2020

A)

Category	Code	Size	Morphology	Definition
Microplastic	PT	5mm-1mm	Pellet	a small spherical piece of plastic less than 5mm to 1mm in diameter
	FR	5mm-1mm	Fragment	an irregular shaped piece of plastic less than 5mm to 1mm in size along its longest dimension
	FB	5mm-1mm	Fiber	a strand or filament of plastic less than 5mm to 1mm in size along its longest dimension
	FI	5mm-1mm	Film	a thin sheet or membrane-like piece of plastic less than 5mm to 1mm in size along its longest dimension
	FM	5mm-1mm	Foam	a piece of sponge, foam or foam-like plastic material less than 5mm to 1mm in size along its longest dimension
Mini-Microplastic	MBD	1mm-1um	Microbead	a small spherical piece of plastic less than 1mm to 1um in diameter
	MFR	1mm-1um	Microfragment	an irregular shaped piece of plastic less than 1mm to 1um in size along its longest dimension
	MFB	1mm-1um	Microfiber	a strand or filament of plastic less than 1mm to 1um in size along its longest dimension
	MFI	1mm-1um	Microfilm	a thin sheet or membrane-like piece of plastic less than 1mm to 1um in size along its longest dimension
	MFM	1mm-1um	Microfoam	a piece of sponge, foam or foam-like plastic material less than 1mm to 1um in size along its longest dimension

B)

Color	Code	Color	Code	Color	Code
any color	***ALL***	dark	**DK**	purple	**PR**
all opaque	***AO***	gold	**GD**	red	**RD**
all transparent	***AT***	green	**GN**	silver	**SV**
amber	**AM**	grey	**GY**	speckled	**SP**
beige	**BG**	ivory	**IV**	tan	**TN**
black	**BK**	light	**LT**	transparent	**TP**
blue	**BL**	metallic	**MT**	turquoise	**TQ**
brown	**BN**	olive	**OL**	violet	**VT**
bronze	**BZ**	opaque	**OP**	white	**WT**
charcoal	**CH**	orange	**OR**	yellow	**YL**

clear	**CL**	pink	**PK**		

Continuing to work in batches, the petri dishes were taken out of storage and assessed one at a time. First, the DC dish was opened, wetted with the volume of DI water determined by Trial Run Treatment 3, then visually assessed based on the methodology outlined above. Once completed, the DC dish was left open to any aerial contamination of the microscope area while the field samples went through the same assessment procedure (wetted & counted) but closed immediately before moving to the next sample. After the rest of the batch was complete, the DC dish was counted again and closed. Petri dishes were then taped closed, and stored in the same manner as before ***(Fig.7)***.

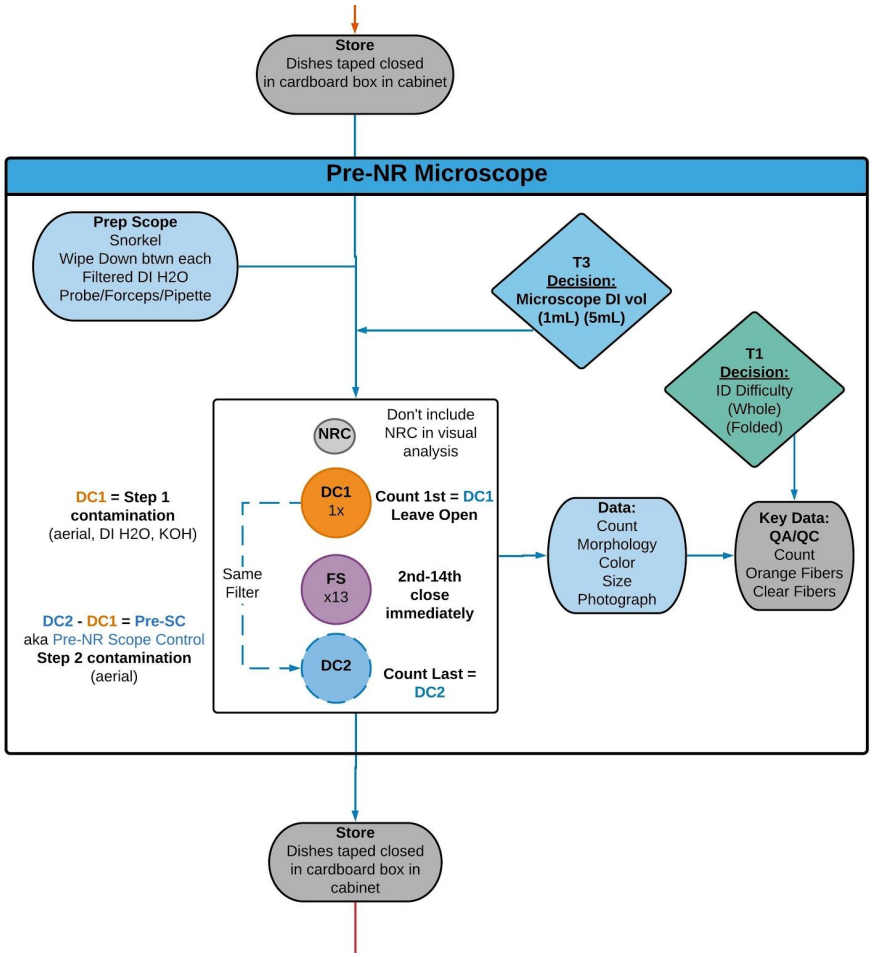

Fig.7 - Concept Map: Pre-Nile Red Microscope Visual Analysis
A chronological flow chart of the first microscope analysis, before Nile Red dye was applied to samples. After the microscope area was prepared according to QA/QC protocols the sample batch (not including NRC) was visually assessed in the order described above. The diamonds represent decisions made from the result of Trial Run Treatments (T1, T3). At this stage, potential contamination was quantified for the exposure to air and lab materials during organic matter digestion (Step 1) as well as by finding the difference between the first and second counts of the DC filter - called the Pre-Nile Red Microscope Control (Pre-SC). Orange and transparent fibers were noted as potential lab coat shedding or conflation with broken filter fibers - at the discretion of Trial Run Treatment 1 results.

3 ◆ *Nile Red Dye*

Nile Red Dye (NR) was selected as the first form of MP validation - a way of fluorescing plastics under dark room conditions among the glass fibers of the filter & any remaining organic matter. This is due to its lipophilic nature, NR is able to attach and dye the hydrocarbons making up the plastic polymers - a characteristic that underscores the importance of removing as much organic matter as possible to

reduce background fluorescence and false positives.[49] In the literature NR has been used in conjunction with micro-FTIR or Raman spectroscopy to validate and quantify visual MP identification confidence, as its sole use is not recommended in the literature.[50]

The dye dilution and application procedure was adapted from Valine (2019) and Wiggin & Holland (2019) ***(Fig.8)***. The NR Stock Solution [1mg NR/mL] was made by dissolving 1mg NR (Catalog# SC-203747B) in 1mL acetone in the fume hood. The NR Stock Solution was then combined with 100mL hexane at room temperature for three hours, covered on a mixing table. Once completed, the NR Working Solution [10µg NR/mL] was transferred into 125mL glass amber dropper bottles to store at 4°C if not used immediately.

Continuing to work in batches, the 15 petri dishes were taken out of storage and moved to the fume hood. First, the empty NRC petri dish was opened and a clean, GF/F filter was placed inside and nine drops (~0.45mL) of NR Working Solution were applied, coating the filter.[51] The dish was left open for the remainder of the batch application, as the field samples and DC each had nine drops applied - after which each dish was closed before moving on to the next. The NRC was then closed at the conclusion of the batch application. The batch was then transferred to the drying oven at 30°C for 12 hours. Once cooled, the petri dishes were stored in the cabinet box as before.

[49] Shim et al., 2016; Stanton et al., 2019; Tamminga et al., 2017; Maes et al., 2017; Erni-Cassola et al., 2017; Cole, 2016
[50] Stanton et al., 2019
[51] Valine, 2019

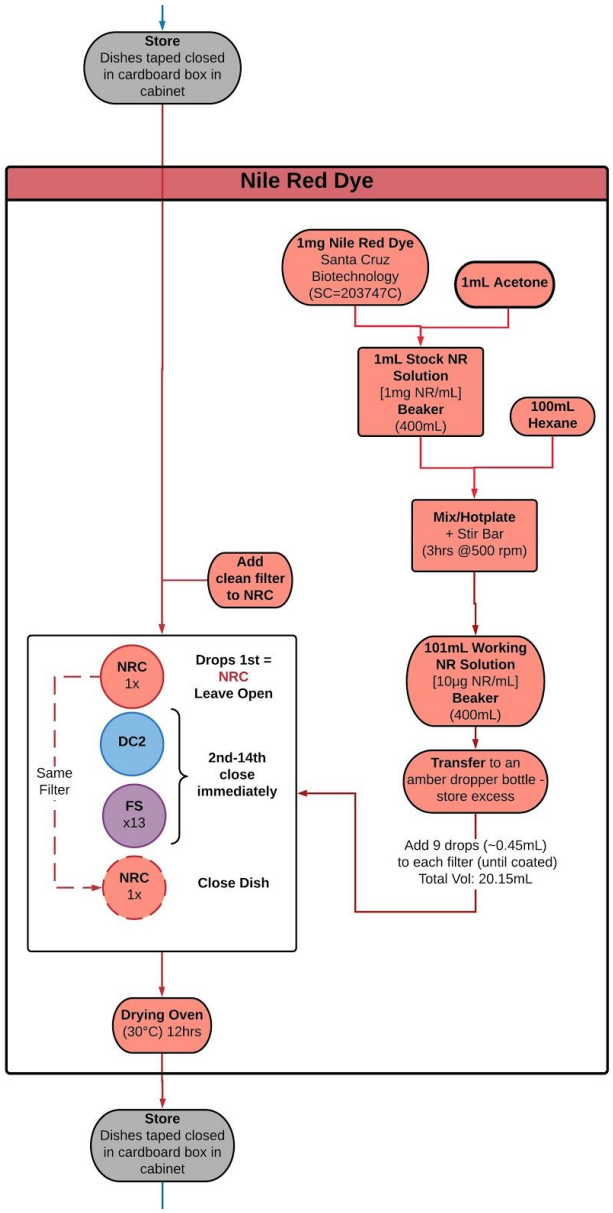

Fig.8 - Concept Map: Nile Red Dye Application

A chronological flow chart of the Nile Red Dye dilution and application process - including the formulation of the NR Stock Solution (1mg NR/mL Acetone) diluted in 100mL Hexane to make the NR Working Solution (10µg NR/mL). Application of the NR Working Solution was conducted on a clean, unwetted filter in the NRC dish, left open to capture potential contamination via aerial deposition as well as from Nile Red dye, Hexane and Acetone materials (quantified in the Post-NR Microscope Visual Analysis step).

4 ◆ *Post-Nile Red Microscope Visual Analysis*

Post-NR set-up used the same microscope area preparation as the Pre-NR steps, including the snorkel and other QA/QC procedures. The area was also amended with dark room/fluorescence conditions including no lights on in the lab, the use of a 455nm flashlight (Arrowhead SKU# A-6994FK), and the associated orange viewing glasses temporarily affixed to the microscope.[52] In so doing, dyed MPs fluoresced and were counted,[53] characterized by morphology, measured and photographed similarly to the Pre-NR microscope visual analysis, ***(Table.3)***, but disregarding the color codes in lieu of dark/fluorescent conditions, an example of which is illustrated well by figure 3 from Valine, 2019,

[52] Valine, 2019
[53] Cole, 2016; Frias et al., 2019; Maes et al., 2017; Prata et al., 2019

(Fig.9).

Fig.9 - Example of Nile Red Fluorescence
The photo in figure 3 of (Valine, 2019) was taken after undergoing the same dye procedure using Nile Red in the same concentration and application methodology as the samples in this survey, including the same Arrowhead 455nm fluorescence flashlight & orange goggle filter kit.

After moving the appropriate batch to the prepared microscope area, the NRC dish was opened and wetted with the volume of DI water determined by Trial Run Treatment 3 (1mL or 5mL) before being counted. The NRC was left open to aerial contamination while the subsequent samples were assessed - closing field and DC samples immediately before moving on to the next. Once the batch was fully assessed, the NRC was counted again under normal lab light and microscope conditions for aerial contamination using Pre-NR characterization methods. Sample petri dishes were then taped closed and returned to room temperature, dark storage conditions ***(Fig.10)***.

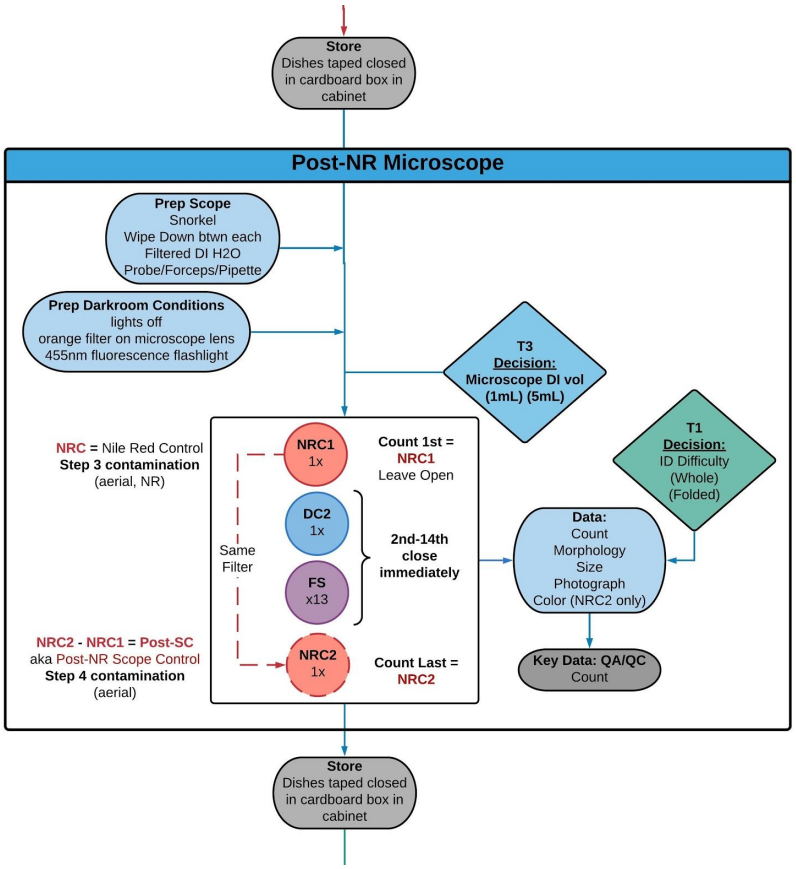

Fig.10 - Concept Map: Post-Nile Red Microscope Visual Analysis & Fluorescence

A chronological flow chart of the second visual microscope analysis via fluorescence of MPs dyed with Nile Red dye. The microscope area underwent previously outlined QA/QC procedures with additional dark room conditions necessary for fluorescence. The NRC was assessed first in the batch, providing quantification of contamination during the Nile Red dye application step - including aerial and from lab solutions (NRC1). After determining NRC1, contamination during Post-NR microscope analysis was quantified by leaving the NRC filter open while the other filters in each batch were analyzed under the microscope. When all other filters were counted, Pre-NR microscope conditions were put in place (no orange light filter, lab lights on) and NRC2 was analyzed according to Pre-NR characterization. This is then used to calculate the Post-NR Microscope Control that quantified aerial contamination that deposited between NRC1 & NRC2 (during batch analysis). The diamonds represent decisions made from the result of Trial Run Treatments (T1, T3).

IV ▸ *Analysis*

5 ◆ *Micro-Fourier Transform Infrared Spectroscopy*

After omitting potential contamination from the compiled MP data pool, in the form of orange fibers and control filters, the labels of all MPs identified on Grays Harbor and La Push filters were randomized and ten percent of them were selected to undergo micro-FTIR validation. Each selected MP was isolated from its filter using the microscope and placed in a small, acrylic vial - submerged in 1mL of 70% ethanol. These samples were then transported to Dr. Brander's lab at Oregon State University for analysis.[54] Before sample analysis, a background calibration scan was run to normalize the instrument to background interference signals from water vapor and carbon dioxide. Then, the scan parameters were input, including the number of scans per sample (no fewer than 20 scans) and the wavenumber range (ATR = 4000-600 cm^{-1}) which includes the fingerprint region of the signal that is unique to the analyzed sample (1450-600 cm^{-1}).[55] Once the background calibration scan was complete, the sample was placed and run according to Dr. Brander's Lab protocols. Each MP's spectrum was automatically compared to the database and a percentage similarity was produced, and accepted if greater than 70% similar to

[54] B. Baechler, personal communication, January 9, 2020
[55] Crawford & Quinn, 2017 (pg.248-249)

reference spectra and if confirmed manually by expert opinion[56] ***(Fig.11)***.

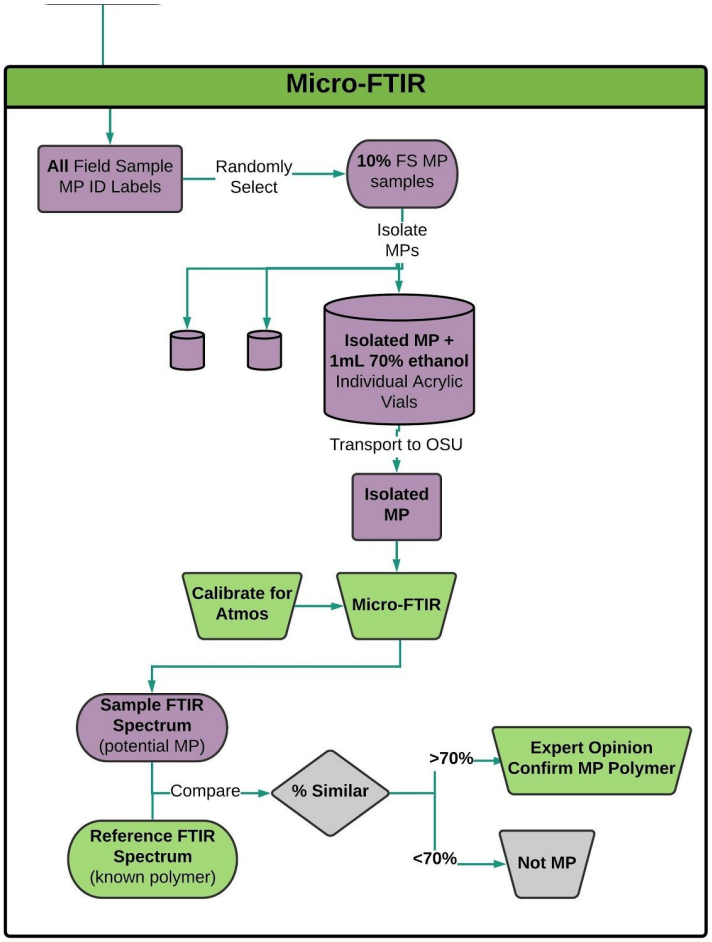

Fig.11 - Concept Map: Micro-FTIR
Chronological flowchart describing the process of field sample MPs (purple) being randomly selected, isolated, and transported to Dr. Brander's Lab (Oregon State University) for Micro-FTIR validation analysis. Each MP was isolated in 1mL filtered 70% ethanol in individual acrylic vials. At OSU the micro-FTIR machine was calibrated for atmospheric interference before each sample before the spectrum of the sample was collected and compared to the library of reference spectra. Once they were compared (% similarity) any below 70% were not validated as MP. Any that met or exceeded 70% were confirmed by expert opinion to rule out interference via biofouling or weathering degradation.

Through this analysis, the polymer type of a representative portion of sea surface MPs was quantified for these two transects through a highly accurate infrared (IR) spectra containing distinct and identifiable band patterns from each MP sample based on the transmittance, reflectance or attenuated total reflection (ATR) of the sample's spectra.[57] These three modes of FTIR microscopy are used in conjunction to identify polymers in comparison to reference spectra in available databases. These data provided useful information regarding potential MP source, input pathway or important characteristics of polymers that may increase interaction with particular environmental conditions. An example spectra for nylon is shown in the top right of ***(Fig.12)***. The bands of IR absorption in each sample's spectrum correspond to the molecular bending and stretching of specific types of polymer functional groups - the characteristic wavelengths of which are outlined in the adapted Crawford & Quinn, 2017, figures below ***(Fig.12)***. This was particularly important when determining potential interference in the FTIR spectra via potential biofouling and weathering of sample MPs in the environment.

[56] Crawford & Quinn, 2017 (pg. 247); Shim et.al., 2017; Corami et al., 2020; Gies et al., 2018
[57] Crawford & Quinn, 2017 (pg.241-245)

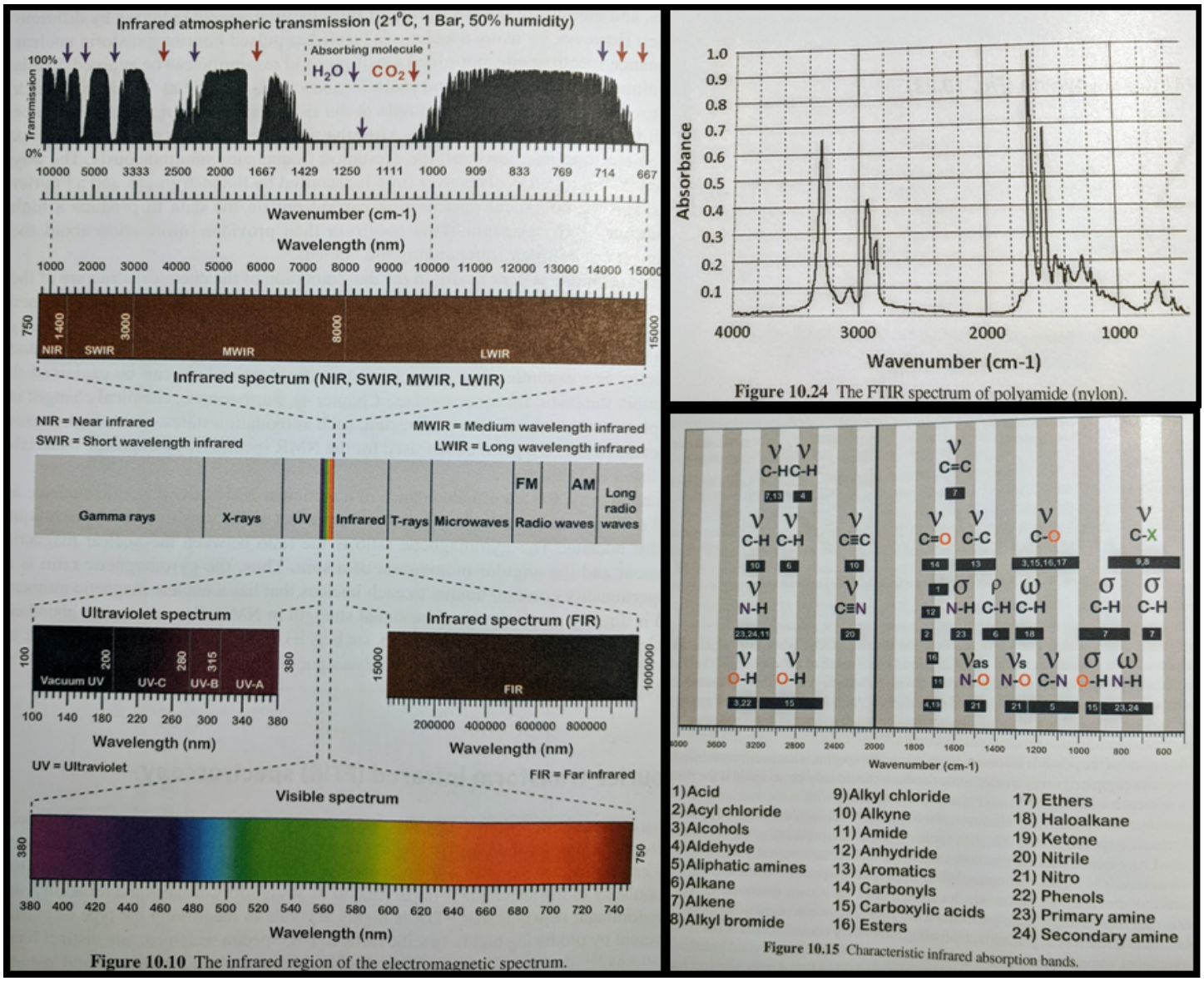

Figure 10.10 The infrared region of the electromagnetic spectrum.

Figure 10.24 The FTIR spectrum of polyamide (nylon).

Figure 10.15 Characteristic infrared absorption bands.

Fig.12 - Micro-FTIR Polymer Readings Structure & Calibration

This figure is collaged from Crawford & Quinn, 2017 (pgs. 242, 248, 254) describing key parts of the polymer spectra reading provided by micro-FTIR analysis. The left (pg.242) shows the range of wavelengths in the infrared region of the electromagnetic spectrum that the signature polymer spectra are found. The top spectrum of the left figure shows an infrared atmospheric transmission reading (calibrated before each sample) under the following conditions: 21°C, 50% humidity, 1 bar atmospheric pressure. Each arrow indicates a wavelength being absorbed by either CO_2 (red) or H_2O vapor (blue). The top right graph (pg.254) is the reference FTIR spectrum for nylon (polyamide), while the bottom right graph (pg.248) maps the characteristic infrared absorption bands for specific types of polymer functional groups (numbered below the graph).

6 ◆ *Statistics*

The data was compiled and cleaned for identification of appropriate statistical assumptions to best analyze the data. To identify any statistically significant relationships between the characterization of MP morphology/polymer type, distribution & abundance, and the sea surface environmental variables during sampling, three major statistical tests were performed. To better identify the influence of local-scale oceanographic conditions, all measured environmental variables from each station will be compared in multiple regressions, t-tests & nMDS statistical tests with MP morphology and polymer distribution & abundance. Multiple regressions were run between the independent (*e.g.,* distance from shore; salinity) and dependent variables (*e.g.,* microfiber abundance; polymer type abundance; size). A

T-test was performed to compare data between transect locations, north vs south. A non-metric multidimensional scaling (NMDS) test was performed to compare the dissimilarity within the multivariate abundance data, as it is particularly suited to spatial/abundance data structure and multifaceted drivers.

V ▸ *Quality Assurance / Quality Control [QA/QC]*

To reduce contamination & maintain the validity of the field samples during lab processing a series of QA/QC measures were taken in the field, during lab work & storage.[58] Standard lab rules were amended to include:

- 100% cotton, orange lab coat & cotton clothing is worn in the lab at all times
- Work surfaces are thoroughly cleaned periodically using 70% ethanol between processing steps/substeps and before/after work at the surface
- Nitrile gloves are worn with each lab processing step & changed between each batch of samples or after touching multiple surfaces
- All materials are washed thoroughly with DI water three times before use & plastic materials were avoided or replaced with glass items
- All containers remain covered when not actively being handled, either by a lid or by aluminum foil
- All fluid materials are filtered using 0.7µm Whatman glass microfiber filters (GF/F) (WHA-1825047)

All fluid materials in the study were individually filtered using the same GF/F filters as field collection & lab processing in order to quantify potential contamination from lab grade chemical sources and materials (filtered sea water, DI water, ethanol, KOH, hexane, and Nile Red working solution). During lab processing, step by step control filter regimes are described in their associated sections and conceptual maps - however, their rationale is summarized in the table below ***(Table.4)***.

Table.4 - Contamination Controls Summary Table

Summary table of the control filter regimes and rationales by processing step, outlining the data controlled for by each. These data is organized describing the data provided by each step, though quantified during one of the microscope visual analyses steps.

**NRC2 analysis was conducted under normal light conditions and described using the methods of Pre-NR microscope analysis*

Processing Step	Control Name	Contamination Controlled For
Field Sampling	EC - Environmental Control	Aerial deposition: Field Sampling
	PC - Procedural Control	Filtered Sea Water Shipboard Seawater Intake System Sieve Tower
Organic Matter Digestion	DC1 - Digestion Control (count 1)	Aerial deposition: KOH application Filtered DI water KOH Digestion Solution
Pre-NR Microscope	Pre-NR Microscope Control	*= (DC2) - (DC1)* Aerial deposition: Pre-NR Microscope Analysis
Nile Red Dye	NRC1 - Nile Red Control (count 1)	Aerial deposition: NR application Nile Red Dye Acetone Hexane
Post-NR	Post-NR Microscope Control*	*= (NRC2) - (NRC1)*

[58] Gies et al., 2018; Hu et al., 2019; Piarulli et al., 2019; Cincinelli et al., 2017; Corami et al., 2020; Dehaut et al., 2016; Hidalgo-Ruz et al., 2012; Maes et al., 2017; Mausra et al., 2015; Michida et al., 2019; Shim et al., 2017

Microscope		Aerial deposition: Post-NR Microscope Analysis*

Expected Results & Discussion

VI ▸ Patterns & Variability in MP Abundance: Drivers

1 ◆ *Transect Location*

Microplastic abundance is expected to have negligible variability between the northern (La Push: 47.92°N) and the southern transect (Grays Harbor: 47.10°N) due to their close proximity in latitude along the Pacific Northwest coast. The MP concentrations from Worm (2017) notate the Pacific Coast as containing 0.00000485 MP/50mL (~0.097 MP/m^3) while the Pacific Gyre concentrations were found to be 0.0001115 MP/50mL (~2.23 MP/m^3) while further south, abundances were notated as 0.0003625 MP/50mL (~7.25 MP/m^3).[59] While these concentrations vary drastically, the distance between each La Push and Grays Harbor (97.93 km between the most inshore stations: GH01b & LP04) won't allow the same level of variability patterns to be seen as those present at scales including the North Pacific Gyre and the California Current. Law (2017) describes, in the figure below, compiled abundance and size data for global surface tows in 2014 - though reported by sea surface area towed (km^2) as opposed to volume of seawater sampled as in this study (L) Fig.13. However, the proportions expected in this study can be contextualized by these coarse scale abundances - such as providing a way to identify outliers within this study's data. These data shows that the pertinent concentrations (top) off the NW coast of Washington, USA, encompassing our sites, are between 104-105 particles/km^2 (0.01-0.1 particles/m^2; yellow). The mass concentrations (bottom) reported for the area including our sample sites is 103-104 g/km^2 (0.000103-0.000104 g/m^2; green). ***(Fig.13)***

[59] Worm et al., 2017 (pg.9)

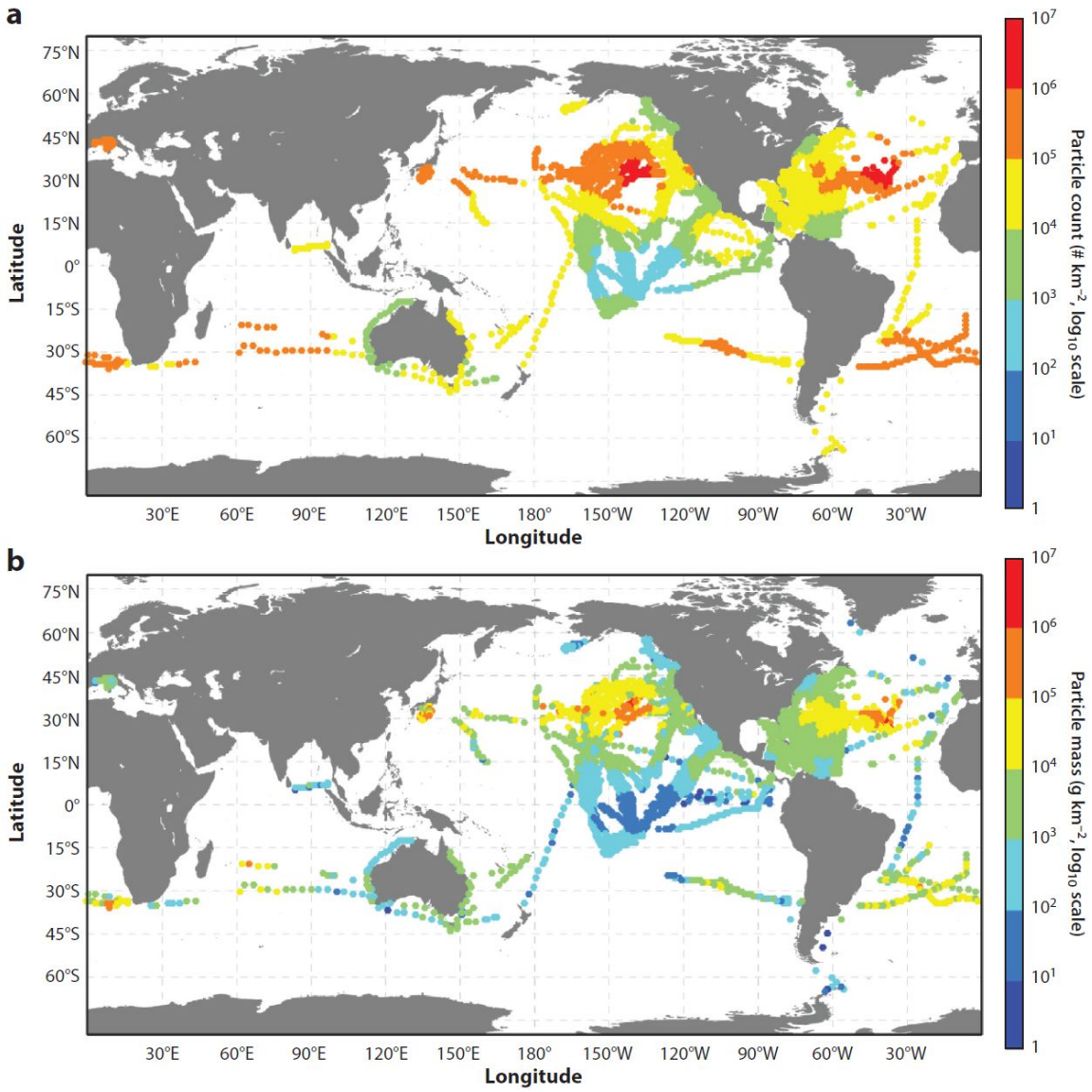

Figure 3

(*a*) Particle count and (*b*) particle mass of plastic samples collected from 11,854 surface-towing plankton net trawls. The data were standardized using a generalized additive model to represent no-wind conditions in the year 2014. Adapted from van Sebille et al. (2015) under the Creative Commons Attribution 3.0 Unported license (**https://creativecommons.org/licenses/by/3.0/legalcode**).

Fig.13 - Global MP Distribution: Abundance & Mass[60]

This figure from Law (2017), summarizes the abundance and mass of sea surface sampling across 11,854 surface tows and modelled on a no-wind model of 2014 microplastic conditions. These data shows that the pertinent concentrations (top) off the NW coast of Washington, USA, encompassing our sites, are between 10^4-10^5 particles/km^2 (0.01-0.1 particles/m^2; yellow). The mass concentrations (bottom) reported for our sample sites is 10^3-10^4 g/km^2 (0.001-0.01 g/m^2; green) While a different reporting factor (by area towed, as opposed to volume sampled) provides a contextual base to identify potential outlier data.

2 ◆ *Distance From Shore*

Based on the literature, the distance from shore is expected to drive more variability in microplastic abundance as Desforges et. al (2014) has shown an explicit inshore-offshore gradient in MP abundance off the west coast of Vancouver and variability ranging from 8-9180 MP/m^3 ***(Fig.14)***. Inshore concentrations were found to be 4-27 times greater than offshore levels. The mean concentration found in the oceanographic region defined as the West Coast of Vancouver Island was found to be 1710 ∓ 1110

[60] Law, 2017 (pg.214)

MP/m^3.[61] This is particularly relevant as the transect sites assessed in this study fall near or within the most southern part of Desforges et al. (2014) study area. However, there's a notable pocket of localized decreased MP abundance to the southwest of Vancouver Island - displaying lower than average coastal concentrations.[62] Based on the data displayed in ***(Fig.14)***, expected concentrations inshore/offshore along Grays Harbor & La Push transects should mimic concentrations between 0-2000 MP/m^3.

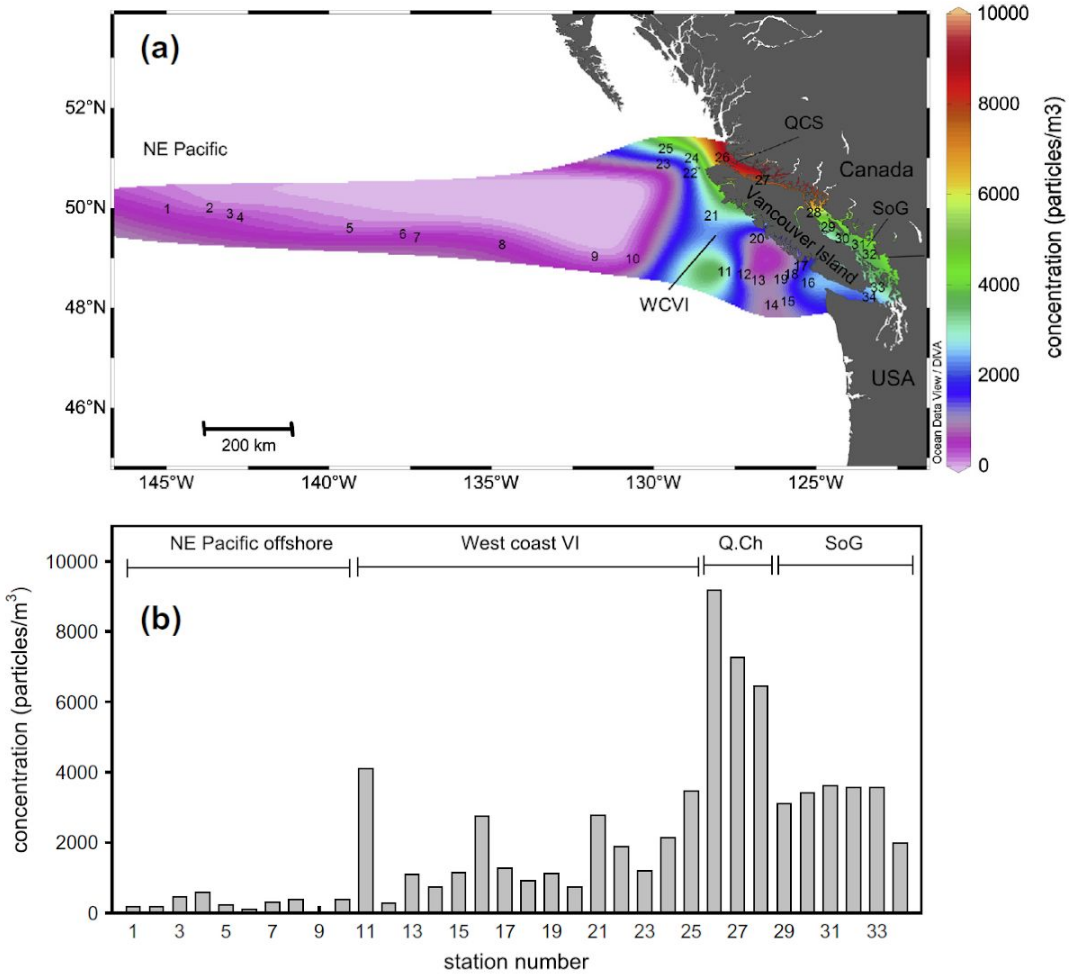

Fig. 1. Total microplastic concentrations (particles/m^3; detected particles >62 µm) in subsurface waters (4.5 m) of the NE Pacific Ocean in and around coastal British Columbia, Canada. (a) Sample locations are numbered (1–34), and the concentration gradient was estimated using DIVA gridding function of Ocean Data View 4. (b) Total microplastic concentrations at each sampling station are grouped into major oceanographic regions for this study: northeastern Pacific Ocean (NE Pacific), west coast Vancouver Island (WCVI), Queen Charlotte Sound (QCS), and Strait of Georgia (SoG).

Fig.14 - NE Pacific Subsurface MP Concentrations[63]
The figure above from Deforges et al. (2014) displays microplastic concentrations (lower limit = 62µm) in the subsurface waters (4.5m) throughout four oceanographic regions in the Pacific Northwest. The one most closely related to the Olympic Peninsula transects addressed in this study is the West Coast of Vancouver Island (WCVI) region - the concentrations of which range from 0-4000 MP/m^3. However, there's a notable pocket of low concentrations to the southwest coast of Vancouver Island.

The oceanographic inshore-offshore exchange during the fall of 2019 was notable due to a late fall transition from upwelling to downwelling as "weak upwelling favorable winds continued through November, which is rare, but also occured in 2013" ***(Fig.15)***.[64] This uncommon continuation, though weak, of upwelling-favorable winds at the Newport Hydrographic line into the late fall indicates potential offshore movement of surface waters, which could dampen a significant MP abundance gradient in 2019 that may usually be present due to fall downwelling transitions moving surface water towards shore -

[61] Desforges et al., 2014
[62] Desforges et al., 2014
[63] Desforges et al., 2014 (pg.96)
[64] Northwest Fisheries Science Center, 2019

pinning MPs against the coast.

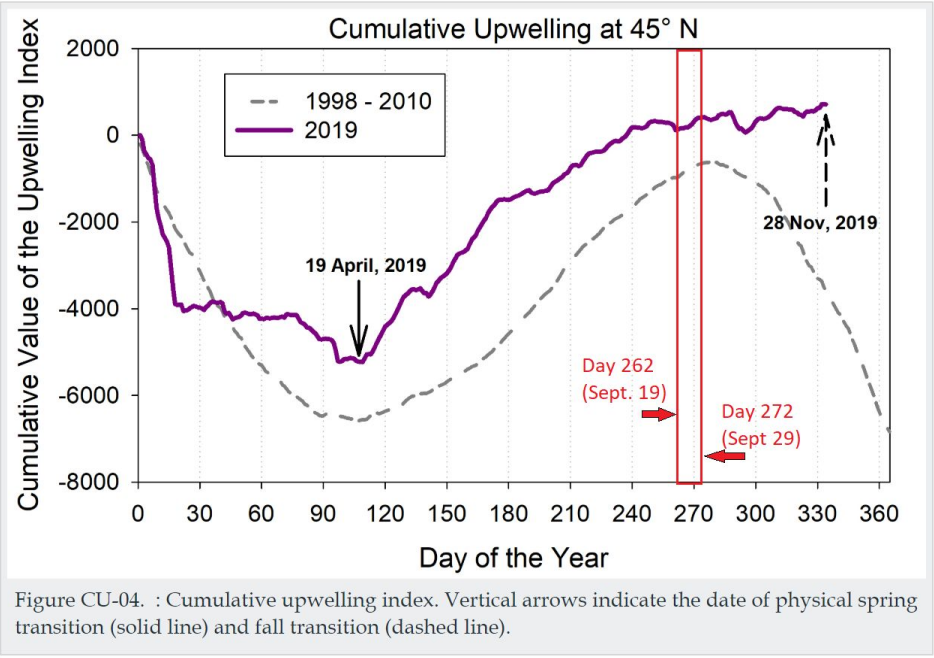

Figure CU-04. : Cumulative upwelling index. Vertical arrows indicate the date of physical spring transition (solid line) and fall transition (dashed line).

Fig.15 - Cumulative Upwelling Index at 45°N [65]

A graph of the cumulative upwelling index along the Newport Hydrographic Line (45°N; long-term NOAA monitoring site) describing the late fall transition along the west coast of Oregon in 2019. While the downwelling period at the beginning of the year was close to the climatological mean, the onset of upwelling (relatively strong) was marked on April 19th, the strength of which decreased mid-June and remained weaker than normal throughout the season. However, it's notable that "weak upwelling favorable winds continued through November, which is rare, but also occured in 2013".[66] *This study's sampling window is indicated by the red box & associated dates on the figure.*

VII ▸ *Patterns & Variability in MP Type: Characterization*

1 ◆ *Morphology*

Microplastic morphology is expected to vary relative to distance from shore - with microfibers being found in greater abundance than any other morphology.[67] The minimum size ranges expected from the sea surface samples in this study is 63µm (smallest mesh size of the sieve tower) while smaller MP may be captured within the range of 0.7µm-63µm from processing contamination or morphologies such as microfiber bundles (compound structures of tangled microfibers accumulating mass) though the lower limit of MP sizes able to be identified under the microscope is expected to be ~0.15mm (~150µm)[68]. The variability in MP sizes expected can be projected based on the literature review of Hidalgo-Ruz et al. 2012, showing sea surface MP size ranges of 53µm-3mm. However, these data is based specifically on particle fragments and the collection & processing methods of each study is directly related to the lower limit of detected MPs ***(Fig.16)***. Desforges et al. (2014) found a size range of 64.8µm-5810µm (5.81mm) with an average size of 606 ∓221µm.

[65] Northwest Fisheries Science Center, 2019
[66] Northwest Fisheries Science Center, 2019
[67] Hidalgo-Ruz et al., 2012 (pg.3065)
[68] Baechler et al., 2019

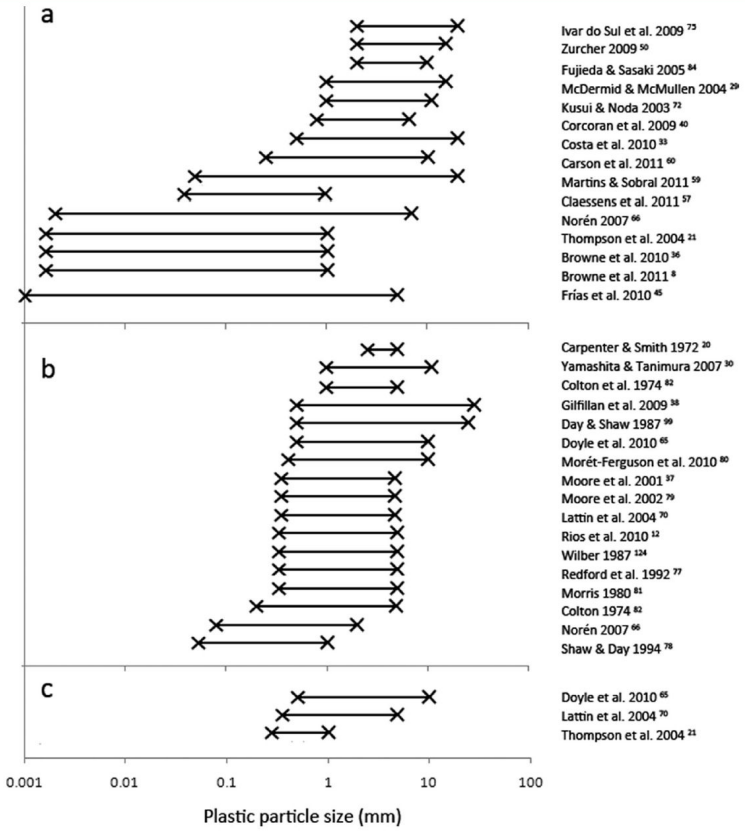

Figure 2. Size ranges for microplastics from (a) sediment, (b) sea surface, and (c) water column studies. Only those studies that provided the lower and upper size limits of microplastics are shown (excluding studies of plastic pellets because here size limits are dictated by pellet sizes).

Fig.16 - MP Size Ranges at Sea Surface[69]

In their literature review of microplastic sampling in the marine environment, Hidalgo-Ruz et al. (2012) constructed the above figure to compare the size ranges found in each environmental compartment (a = sediment; b = sea surface; c = water column) the 68 studies they reviewed reported. Examining the central plot (b = sea surface; number of studies = 17), the range in MP size was 0.5µm-29mm. However, it is notable that this plot only includes particles (or fragments as they're also known) and doesn't address microfibers or the bundles they may form as they weather and move in the environment. Additionally, the minimum size of the collected MP is directly dependent on each study's collection & processing methodology - for example seawater bulk sample mesh nets varied from 53µm-3mm while their filter pore size limited collection of MPs smaller than 1.6-2µm.

Microfibers are expected to exceed other morphologies in proportions (~70-80% of MPs) off the Olympic Peninsula based on data from Desforges et al. (2014) research off the west coast of Vancouver Island & northern Washington ***(Fig.17)***. This is supported by recent research regarding the proportions of estimated MP release based on source & morphology showing higher overall release of microfibers from anthropogenic sources like household synthetic textiles.[70] Desforges et al. (2014) found that three-quarters of their MP samples were microfibers and that overall MP sizes increased linearly from the coast to 600km offshore.

[69] Hidalgo-Ruz et al., 2012 (pg.3065)
[70] Boucher & Friot, 2017; Falco et al., 2019; Henry et al., 2019

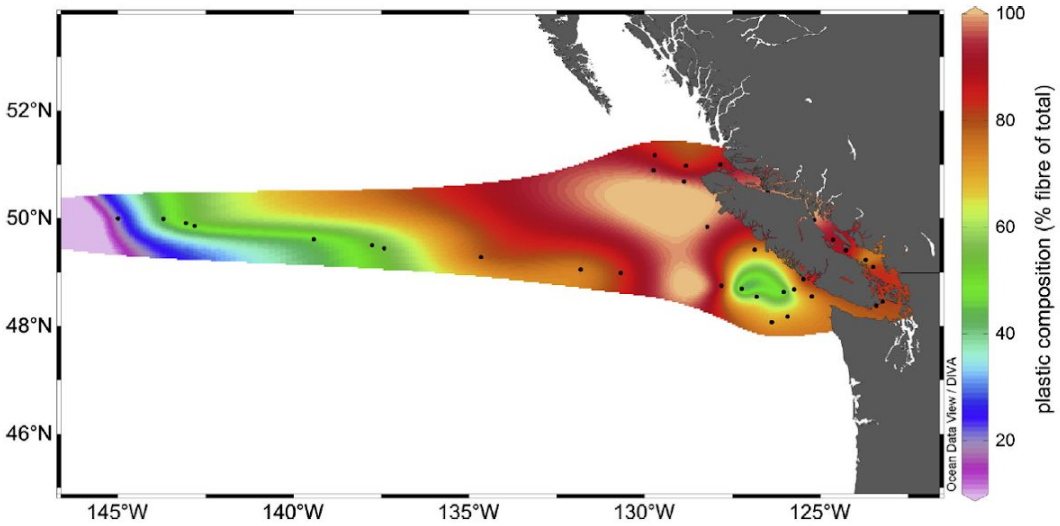

Fig. 2. Map of microplastic composition, defined here as a percentage fibre of the total plastics detected. Sampling stations are depicted as black dots. Values have been estimated using the DIVA gridding function of Ocean Data View 4.

Fig.17 - MP Concentration: Percent Microfibers[71]

Desforges et al. (2014) were able to describe their estimated MP composition (using the DIVA gridding function of Ocean Data View 4) to show the percentage of microfibers they found in their abundance counts. The area relevant to this study includes the Olympic Peninsula, showing proportions of ~70-80% microfibers of all the MP they found at those sites. This indicates that similar patterns & proportions may be found in this study.

2 ◆ Polymer Composition

Abundance patterns by polymer composition is expected to follow a higher proportion of low density polymers, based on relative buoyancy in sea water conditions ***(Table.5)*** - as some MPs have been found to aggregate in different compartments of the environment based on a number of factors, including density/buoyancy ***(Fig.19)***.[72] The polymer groups expected to make up the majority of sea surface MP due to this important factor include: polystyrene (PS), polypropylene (PP), low density polyethylene (LPDE), ethylene vinyl acetate (EVA), and high density polyethylene (HDPE) ***(Table.5)***.[73] This doesn't preclude the presence of higher density plastics, particularly at stations where weather conditions were particularly turbid, low temperature, or those where upwelling influence remains present - pushing higher density MPs to the surface.

Table.5 - Polymer Density & Buoyancy in Seawater[74]

A table from Frias et al. (2019) describing the buoyancy relationships between different MP polymer types in seawater (density = 1.025 g/cm^3). While this is a generalized model as polymer density may be shifted slightly due to additives and the seawater changes density based on temperature and salinity. However, this can provide a tentative guide to what types of polymers may be more likely to be present within 2-3 meters of the surface.

[71] Desforges et al., 2014 (pg.97)
[72] Frias et al., 2019; Baechler et al., 2019; Brandon, 2017; Desforges et al., 2014; Isobe et al., 2014; Law, 2017; Leslie et al., 2017; Li et al., 2018; Shim et al., 2017; Wardrop et al., 2016; Worm et al., 2017
[73] Frias et al., 2019
[74] Frias et al., 2019 (pg.24)

Abbreviation	Polymer	Density (g cm^{-3}) *	Buoyancy
PS	Polystyrene	0.01 – 1.06	Positive (↑)
PP	Polypropylene	0.85 – 0.92	Positive (↑)
LDPE	Low-density polyethylene	0.89 – 0.93	Positive (↑)
EVA	Ethylene vinyl acetate	0.93 - 0.95	Positive (↑)
HPDE	High-density polyethylene	0.94 – 0.98	Positive (↑)
Seawater		**1.025**	
PA	Polyamide	1.12 – 1.15	Negative (↓)
PA 6,6	Nylon 6,6	1.13 – 1.15	Negative (↓)
PMMA	Poly methyl methacrylate	1.16 – 1.20	Negative (↓)
PC	Polycarbonate	1.20 – 1.22	Negative (↓)
PU	Polyurethane	1.20 – 1.26	Negative (↓)
PET	Polyethylene terephthalate	1.38 – 1.41	Negative (↓)
PVC	Polyvinyl chloride	1.38 – 1.41	Negative (↓)
PTFE	Polytetrafluoroethylene	2.10 – 2.30	Negative (↓)

Polymer density might vary with additives added during production.

3 ◆ *Transect Location*

While transect location, either the northern (47.92°N) or southern (47.10°N) latitude may be a minor driving factor due to the study sites' proximity to the Salish Sea & Juan de Fuca to the north, it is not expected to be as impactful as distance from shore in morphological or polymer variability. This is due to the small scale of their relative distance compared to the oceanographic systems & seasonal coastal upwelling influences along the west coast - only about 98km separate the most inshore stations of each transect.[75]

4 ◆ *Distance From Shore*

An inshore-offshore gradient pattern is expected to arise out of the abundance and characterization distributions - though perhaps more strongly seen in morphology & size than polymer type. This gradient was initially expected based on the normal seasonal shift in upwelling & downwelling along the west coast, which has usually transitioned to downwelling by September.[76] However, in 2019 there was an unexpected extension of seasonal wind conditions that favored weak upwelling ***(Fig.15)***. Winds that favor downwelling conditions would push surface water movement towards shore, potentially pinning a number of MP against the coast more readily & displaying a drastic gradient. However, this potential gradient may be less present in 2019 specifically due to the late fall downwelling transition, with unseasonable winds pushing surface waters farther offshore - thereby obfuscating patterns in specific MP mobility patterns based on their morphology and polymer type.

There's also reason to expect potential increases nearshore due to proximity to terrestrial outlets of MP contamination pathways (river mouths, wwtp outlets, coastal urban centers).[77] Deforges et al. (2014) found 4-27 times more MP nearshore than offshore, and the size increased linearly away from the coast - though their study included a 600km gradient, far longer than possible in this study and so they

[75] NOAA: National Centers for Environmental Information (formerly the National Climatic Data Center), 2020; Northwest Fisheries Science Center, 2019; Puget Sound Institute, 2007

[76] NOAA: National Centers for Environmental Information (formerly the National Climatic Data Center), 2020; Northwest Fisheries Science Center, 2019; Puget Sound Institute, 2007

[77] Anbumani & Kakkar, 2018; Boucher & Friot, 2017; Carr et al., 2016; Cincinelli et al., 2017; Di Mauro, 2017; Falco et al., 2019; Gies et al., 2018; Granek et al., 2016; Horn et al., 2019; Kedzierski et al., 2019; Kettner et al., 2019; Law, 2017; Leslie et al., 2017; Li et al., 2018; Mason et al., 2016; McCormick et al., 2014; Michielssen et al., 2016; OR&R Marine Debris Division, 2015; Profita & Burns, 2019; Raju et al., 2018; Ryan, 2015; Scherer et al., 2017; Simmerman & Coleman Wasik, 2019; Sun et al., 2019; Wardrop et al., 2016; Worm et al., 2017; Wu et al., 2018

perhaps had a larger scale on which to more clearly identify patterns.

VIII ▸ *Environmental Factors: Correlations with Distribution & Abundance*

A positive trend in abundance of microplastics inshore is expected compared to farther offshore due to the representation of similar local patterns in the literature.[78] The historical seasonal patterns in downwelling/upwelling off the Olympic Peninsula combined with the potential influence of the southeast expansion of the Aleutian Low on sea surface, contributes to "onshore flow into the Pacific Northwest from October through early spring". ***(Fig.18)***[79] However, due to the late September sampling in 2019 and the coinciding late seasonal shifts in large scale surface wind patterns that favored weak inshore movement, this pattern may be masked by uncommon environmental circumstances ***(Fig.15)***.[80]

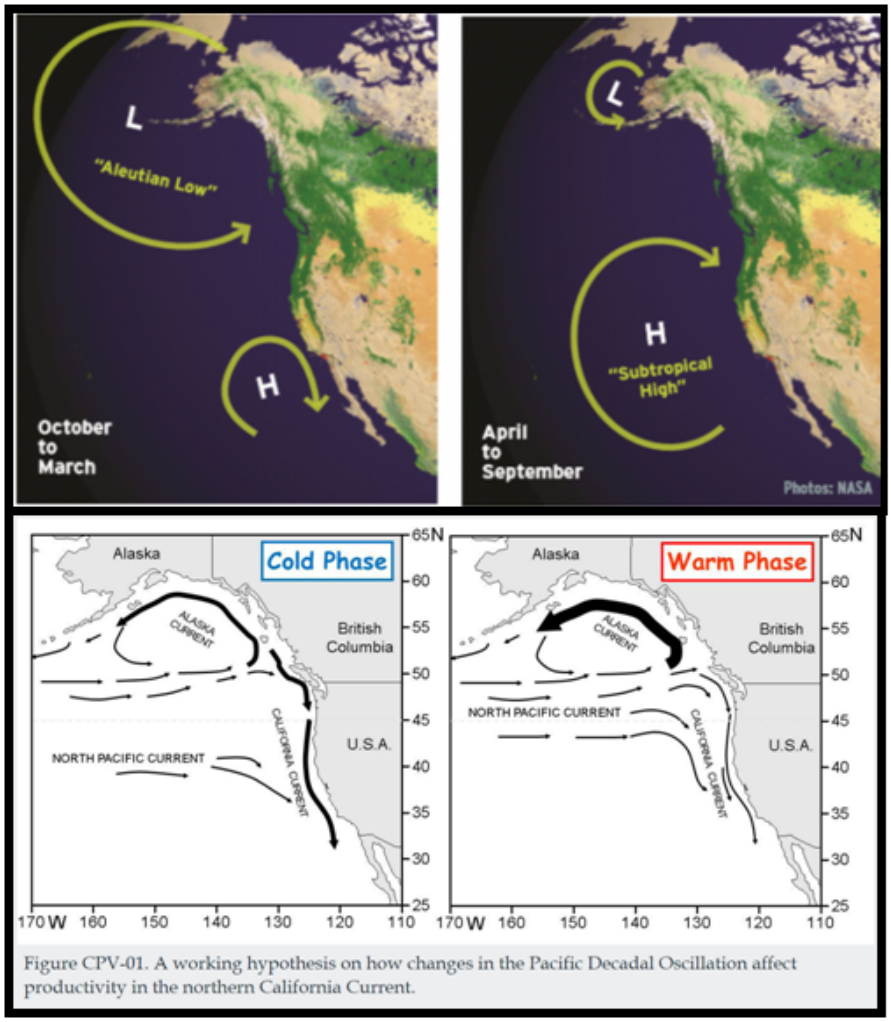

Figure CPV-01. A working hypothesis on how changes in the Pacific Decadal Oscillation affect productivity in the northern California Current.

Fig.18 - Aleutian Low & Pacific Decadal Oscillation[81]
The figures above describe the large-scale seasonal (top, as presented by the Encyclopedia of Puget Sound) and decadal (bottom, as presented by the Northwest Fisheries Science Center) ocean circulation conditions found off the northwest coast of North America. ***Top:*** *The winter (Oct-Mar) conditions of the PNW oceanic atmosphere & sea surface wind movement (direction/scale displayed by yellow arrows) is directly linked to the intensification of the northern semi-permanent Aleutian Low pressure cell and its movement SE seasonally. The migrating low pressure surface winds (counter-clockwise) conflict with the clockwise surface winds of the semi-permanent southern Subtropical High off the southern coast of California, bringing typically "moist, mild, onshore flow into the Pacific Northwest". The transition to summer conditions (April-Sept) shows a strong reduction of landfalling storms as the Subtropical High expands northward and intensifies. These inshore-offshore shifts in sea surface*

[78] Desforges et al., 2014
[79] Puget Sound Institute, 2007
[80] Puget Sound Institute, 2007; Northwest Fisheries Science Center, 2019
[81] Puget Sound Institute, 2007; Northwest Fisheries Science Center, 2019

movement and turbidity state likely have direct impacts on MP distribution & abundance. ***Bottom:*** *By exploring the current state of the Pacific Decadal Oscillation (PDO), one may be able to identify broad scale drivers of MP abundance and distribution based on ocean current mobility & the associated shifts in marine water conditions. The same conditions that shift as indicators of the PDO phase may directly impact MPs including local sea surface temperatures and the salinity of water on the continental shelf, both factors in MP distribution vertically in the water column. During cold phases, the continental shelf is cold and salty, while warm phases bring warm fresh water to the continental shelf. As seen in the figure, the PDO drastically shifts ocean current directionality and intensity (indicated by the black arrows), likely to move MP with them.*

Oceanographic wave dynamics have a direct impact on MP dispersal horizontally along the sea surface & vertically through the water column, as Isobe et al. (2014) visualized in ***(Fig.19)***. In the figure below, their conceptual framework (left) outlines the factors involved in marine mobility of MP and larger mesoplastics, including: buoyancy, friction and wind waves, Stokes drift and depth. .[82] By applying environmental data from on site & these buoyancy-dispersion theories[83] to our characterized MP polymer type distribution & buoyancy profiles, we may be able to explain the variability in MP polymer presence given oceanographic conditions at the time of sampling. In the Seto Inland Sea of Japan, Isobe et al. (2014) were able to interpret potential selective near-shore trapping of larger mesoplastic fragments (>5mm) drifting closer to the surface than smaller MP due to their individual terminal velocity, the larger the fragment the greater terminal velocity. This means smaller MPs may drift lower in the water column than larger mesoplastics in highly turbid surface water, allowing them to escape the strongest forces of Stokes drift at the surface, which the authors reproduced using the model shown in ***(Fig.19)***. These findings may conflict with the findings of Desforges et al. (2014), where larger MP were found farther offshore, likely due to Isobe et al. (2014)'s study location being unique to Japan's oceanography - as the tendency for the western coasts of continents to experience upwelling, while eastern coasts experience far less.

[82] Isobe et al., 2014
[83] Isobe et al., 2014; Brandon, 2017; Crawford & Quinn, 2017

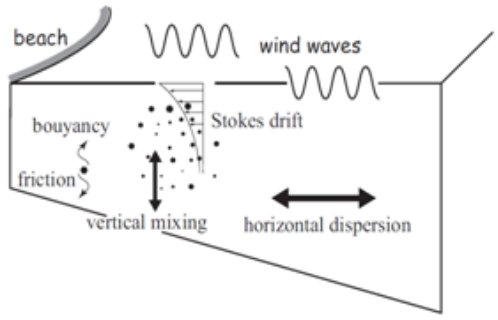

Fig. 5. Schematic view of the selective onshore transport of mesoplastics. See Section 4.1 for details.

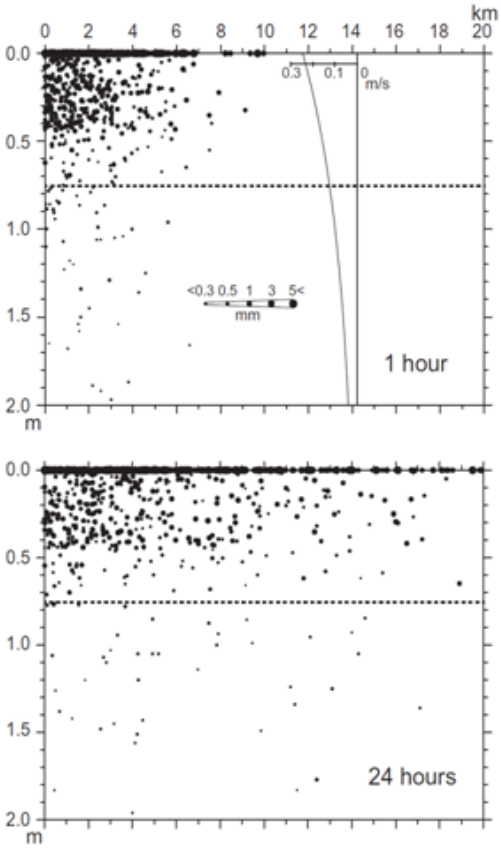

Fig. 6. Modeled particle positions after 1 h (upper panel) and 24 h (lower panel), in the upper 2-m layer of the model domain. The diameters of the particles denote the modeled sizes as shown in the upper panel. The broken line indicates the depth of 0.75 m above which particles were chosen to depict the modeled drift-density map in Fig. 7. Also shown in the upper panel is the current profile of the Stokes drift given to the model.

Fig.19 - Selective Onshore Transport[84]

These figures from Isobe et al. (2014) describe a conceptual (left) and numerical (right) model explaining the seeming selective near-shore trapping of larger mesoplastic fragments (>5mm) but not microplastics in the Seto Inland Sea of Japan. To the right, their drift-density map model displays the way varied sized MP fragments (0.3mm, 0.5mm, 1mm, 3mm, 5mm) disperse horizontally and vertically with Stokes drift accounted for after an hour (right top) and 24 hours (right bottom). According to the model, mesoplastics drift closer to the surface than smaller MP in highly turbid water due to their individual terminal velocity (the larger the fragment the greater terminal velocity). This means smaller MPs may drift lower in the water column than larger mesoplastics, allowing them to escape the strongest forces of Stokes drift at the surface and thereby near-shore trapping forces. However, as the PNW has unique seasonal upwelling patterns, the influence of these variables has not yet been articulated for our site area as opposed to Japan.

The influence of environmental variables & sea surface dynamics will be assessed to identify the magnitude of their influence on the presence of particular sizes or morphologies of MP found, as well as polymer types of particular densities. However, the following environmental variables have been identified in the literature[85] as highly impactful on MP distribution and abundance. Wind speed and direction, combined with seasonality of sampling directly impact the state of wave height and direction at the sea surface, potentially shifting present MP abundance and distribution. MP presence and concentration has shown historical patterns related to distance from shore, potentially due to proximity to river estuaries, or waste water treatment plants. Other sea surface conditions encompass a number of environmental variables that influence MP variability, as identified in the literature: salinity (practical salinity unit; g/kg), sea surface temperature (°C), dissolved oxygen (mg/L or ppm), chlorophyll-a (percent full scale fluorescence ; % FS; or µg/L chlorophyll-a) and the maximum depth in the water

[84] Isobe et al., 2014 (pg.328-329)
[85] Frias et al., 2019; Brandon, 2017

column at which chlorophyll-a is found.[86]

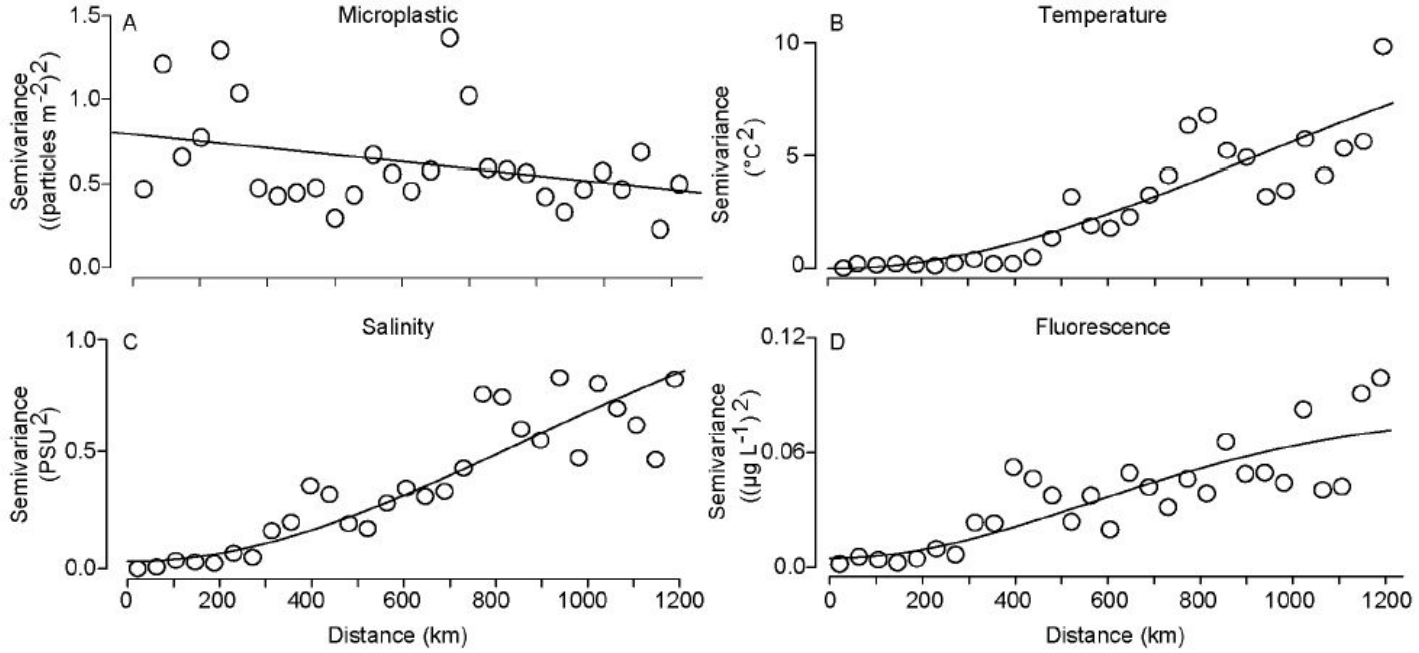

Figure 4. Scale-dependence of variance in microplastic concentration and surface biophysical variables. A) Microplastic numerical concentration; B) Sea surface temperature; C) Sea surface salinity; D) Sea surface fluorescence. Dots are the values of the empirical semivariogram and the lines are a description of the data trends. A is fitted with a linear model, and B–D with Gaussian models. Data are shown for Summer 2009 only since sample size in Fall 2010 was insufficient for this analysis.
doi:10.1371/journal.pone.0080020.g004

Fig.20 - Relationships Between MP Concentration & Sea Surface Biophysical Variables[87]
The Goldstein et al. (2013) figures above describe the variance in A) MP concentration of abundance; B) sea surface temperature; C) sea surface salinity; D) sea surface fluorescence for the summer of 2009 within the North Pacific Subtropical Gyre (~20-40°N, 120-155°W). The semivariance of temperature, salinity and fluorescence increased with distance between sampling sites - meaning that "samples taken closer together were more similar to each other than samples taken farther apart".

Conclusion

IX ▸ *Contamination & Validation*

Using the previously outlined lab rules & QA/QC protocols, contamination was kept to a minimum from numerous potential avenues and quantified using the control filter regime described in ***(Table.4)*** to identify potential sources of interference at each step. To make identification of aerial deposition of contamination easier, all orange fibers were attributed to processing interference from the 100% cotton, orange clothing worn by researchers in the field and lab. The results of Trial Run Treatment 1 qualified the ease with which the folded and broken glass borosilicate microfiber filter could be misidentified as transparent microplastic microfibers under visual microscope procedures. Unfortunately, it's possible these steps may result in a slight underestimation in MP abundance, particularly of microfibers.

However, as much as this project aims to describe the spatial distribution of characterized microplastics off the Olympic Peninsula, it also serves to provide an integrated, tiered structure of contamination control & validation methodology with a range of accessibility in financial terms. By using

[86] Goldstein et al., 2013; Frias et al., 2019; Brandon, 2017
[87] Goldstein et al., 2013 (pg.7)

Nile Red as an intermediate step of quality control, and micro-FTIR analysis to validate the magnitude of error in MP reporting using only visual ID and Nile Red dye, this project provides a stepping stone for standardized MP methodology.

X ▸ *Potential Contributions, Limitations & Future Research*

By characterizing the distribution of microplastics by morphology and polymer type, the potential relationships between MP mobility and the Olympic Peninsula sea surface environmental variables may be elucidated - providing vital information to contextualize the scope of this novel, anthropogenic contaminant. The scope of this project is limited by the scope of logistic processing *in situ* at each station as time restrictions made it impossible to collect three subsamples at every station on each transect as was planned. This left the dataset with seven stations per transect, and fifteen total subsamples for Grays Harbor while La Push included twenty total subsamples. Additionally, any characterization of a PNW baseline is a snapshot of potentially vastly mobile, novel contaminants through marine ecosystem compartments. The final results would be greatly strengthened by the addition of seasonal sampling through time. That being said, the characterization of MPs along these transects sets a foundation for potential long term monitoring by NOAA, or other interested groups, and the beginning of an increasingly important long-term dataset as our anthropogenic impact continues to accumulate.

Acknowledgements

Thank you to my advisor, Dr. Elise Granek, and the entirety of the Applied Coastal Ecology lab at Portland State University for your experience and advice at every point of the development, processing and written phases of this project. Thank you to the wonderful NOAA & Scientific Ops crews of the Bell M. Shimada research vessel as well as Dr Brander's lab at Oregon State University for your valuable partnership to make this research a reality. Thank you to the Ed and Olive Bushby Scholarship Fund and University Honors scholarship program at Portland State University for making the scope of this research accessible where it wasn't otherwise as well as to my family for reminding me it was within my grasp. Most of all, thank you to my senior editor Kat Milano for your keen eyes, wisdom, and patience when mine was wearing thin.

Works Cited

1. Anbumani, S., & Kakkar, P. (2018). Ecotoxicological effects of microplastics on biota: A review. *Environmental Science and Pollution Research International; Heidelberg*, *25*(15), 14373–14396. http://dx.doi.org/10.1007/s11356-018-1999-x
2. Baechler, B. (2019). *Microplastics in Oregon Bivalves Project—Organic Matter Digestion Methodology*. Britta Baechler - Applied Ecology Lab.
3. Baechler, B. (2020, January 9). *Britta Baechler: Microplastic Organic Matter Digestion & Microscope Visual ID Methodology* [Personal communication].
4. Baechler, B. R., Granek, E. F., Hunter, M. V., & Conn, K. E. (2019). Microplastic concentrations in two Oregon bivalve species: Spatial, temporal, and species variability. *Limnology and Oceanography Letters*. https://doi.org/10.1002/lol2.10124
5. Baechler, B. R., Stienbarger, C. D., Horn, D. A., Joseph, J., Taylor, A. R., Granek, E. F., & Brander, S. M. (2019). Microplastic occurrence and effects in commercially harvested North American finfish and shellfish: Current knowledge and future directions. *Limnology and Oceanography Letters*. https://doi.org/10.1002/lol2.10122
6. Bolm, A., & Wood, R. (2019). *Anna Bolm: Sampling Methods Consultation & Collaboration in the Field (Bell M. Shimada—Sept. 2019)* [Personal communication].
7. Boucher, J., & Friot, D. (2017). *IUCN Primary Microplastics In the Oceans: A Global Evaluation of Sources*. International Union for Conservation of Nature, Gland, Switzerland.

https://storyofstuff.org/wp-content/uploads/2017/02/IUCN-report-Primary-microplastics-in-the-oceans.pdf

8. Brandon, J. (2017). *The distribution of suspended microplastics and nanoplastics in the Northeast Pacific and their effects on zooplankton consumers* [UC San Diego]. https://escholarship.org/uc/item/2f3991m5
9. Carr, S. A., Liu, J., & Tesoro, A. G. (2016). Transport and fate of microplastic particles in wastewater treatment plants. *Water Research*, *91*, 174–182. https://doi.org/10.1016/j.watres.2016.01.002
10. Cincinelli, A., Scopetani, C., Chelazzi, D., Lombardini, E., Martellini, T., Katsoyiannis, A., Fossi, M. C., & Corsolini, S. (2017). Microplastic in the surface waters of the Ross Sea (Antarctica): Occurrence, distribution and characterization by FTIR. *Chemosphere*, *175*, 391–400. https://doi.org/10.1016/j.chemosphere.2017.02.024
11. Cole, M. (2016). A novel method for preparing microplastic fibers. *Scientific Reports*, *6*(1). https://doi.org/10.1038/srep34519
12. Cole, M., Webb, H., Lindeque, P. K., Fileman, E. S., Halsband, C., & Galloway, T. S. (2014). Isolation of microplastics in biota-rich seawater samples and marine organisms. *Scientific Reports*, *4*, 4528. https://doi.org/10.1038/srep04528
13. Corami, F., Rosso, B., Bravo, B., Gambaro, A., & Barbante, C. (2020). A novel method for purification, quantitative analysis and characterization of microplastic fibers using Micro-FTIR. *Chemosphere*, *238*, 124564. https://doi.org/10.1016/j.chemosphere.2019.124564
14. Dehaut, A., Cassone, A.-L., Frere, L., Hermabessiere, L., Himber, C., Rinnert, E., Riviere, G., Lambert, C., Soudant, P., Huvet, A., Duflos, G., & Paul-Pont, I. (2016). Microplastics in seafood: Benchmark protocol for their extraction and characterization | Elsevier Enhanced Reader. *Environmental Pollution*, *2015*, 223–233. https://doi.org/10.1016/j.envpol.2016.05.018
15. Desforges, J.-P. W., Galbraith, M., Dangerfield, N., & Ross, P. S. (2014). Widespread distribution of microplastics in subsurface seawater in the NE Pacific Ocean. *Marine Pollution Bulletin*, *79*(1), 94–99. https://doi.org/10.1016/j.marpolbul.2013.12.035
16. Di Mauro, R. (2017). Abundant plankton-sized microplastic particles in shelf waters of the northern Gulf of Mexico. *Environmental Pollution*, *230*. https://www.researchgate.net/publication/318653043_Abundant_plankton-sized_microplastic_particles_in_shelf_waters_of_the_northern_Gulf_of_Mexico
17. EMD Millipore Corp. (2015). *Chemical Compatibility of Filter Components* (p. 16) [Data Sheet]. EMD Millipore Corp.
18. Erni-Cassola, G., Gibson, M. I., Thompson, R. C., & Christie-Oleza, J. A. (2017). Lost, but Found with Nile Red: A Novel Method for Detecting and Quantifying Small Microplastics (1 mm to 20 μm) in Environmental Samples. *Environmental Science & Technology*, *51*(23), 13641–13648. https://doi.org/10.1021/acs.est.7b04512
19. Falco, F. D., Pace, E. D., Cocca, M., & Avella, M. (2019). The contribution of washing processes of synthetic clothes to microplastic pollution. *Scientific Reports*, *9*(1), 1–11. https://doi.org/10.1038/s41598-019-43023-x
20. Frias, J., Filgueiras, A., J. Gago, Pedrotti, M. L., Suaria, G., Tirelli, V., Andrade, J., Nash, R., O'Connor, I., Lopes, C., Caetano, M., Raimundo, J., Carretero, O., Viñas, L., Antunes, J. C., Bessa, F., Sobral, P., Goruppi, A., Aliani, S., … Gerdts, G. (2019). Standardised protocol for monitoring microplastics in seawater. *Unpublished*. https://doi.org/10.13140/rg.2.2.14181.45282
21. Gies, E. A., LeNoble, J. L., Noël, M., Etemadifar, A., Bishay, F., Hall, E. R., & Ross, P. S. (2018). Retention of microplastics in a major secondary wastewater treatment plant in Vancouver, Canada. *Marine Pollution Bulletin*, *133*, 553–561. https://doi.org/10.1016/j.marpolbul.2018.06.006
22. Goldstein, M. C., Titmus, A. J., & Ford, M. (2013). Scales of Spatial Heterogeneity of Plastic Marine Debris in the Northeast Pacific Ocean. *PLoS ONE*, *8*(11), e80020. https://doi.org/10.1371/journal.pone.0080020
23. Gorokhova, E. (2015). Screening for microplastic particles in plankton samples: How to integrate marine litter assessment into existing monitoring programs? *Marine Pollution Bulletin*, *99*(1), 271–275. https://doi.org/10.1016/j.marpolbul.2015.07.056
24. Granek, E. F., Brander, S. M., & Holland, E. B. (2020). Microplastics in aquatic organisms: Improving understanding and identifying research directions for the next decade. *Limnology and Oceanography Letters*, *5*(1), 1–4. https://doi.org/10.1002/lol2.10145
25. Granek, Elise F., Conn, K. E., Nilsen, E. B., Pillsbury, L., Strecker, A. L., Rumrill, S. S., & Fish, W. (2016). Spatial and temporal variability of contaminants within estuarine sediments and native Olympia oysters: A contrast between a developed and an undeveloped estuary. *Science of The Total Environment*, *557–558*, 869–879. https://doi.org/10.1016/j.scitotenv.2016.03.043
26. Harrison, X. A., Donaldson, L., Correa-Cano, M. E., Evans, J., Fisher, D. N., Goodwin, C. E. D., Robinson, B. S., Hodgson, D. J., & Inger, R. (2018). A brief introduction to mixed effects modelling and multi-model inference in

ecology. *PeerJ*, *6*. https://doi.org/10.7717/peerj.4794

27. Henry, B., Laitala, K., & Klepp, I. G. (2019). Microfibres from apparel and home textiles: Prospects for including microplastics in environmental sustainability assessment. *Science of The Total Environment*, *652*, 483–494. https://doi.org/10.1016/j.scitotenv.2018.10.166

28. Herrera, A., Garrido-Amador, P., Martínez, I., Samper, M. D., López-Martínez, J., Gómez, M., & Packard, T. T. (2018). Novel methodology to isolate microplastics from vegetal-rich samples. *Marine Pollution Bulletin*, *129*(1), 61–69. https://doi.org/10.1016/j.marpolbul.2018.02.015

29. Hidalgo-Ruz, V., Gutow, L., Thompson, R. C., & Thiel, M. (2012). Microplastics in the marine environment: A review of the methods used for identification and quantification. *Environmental Science & Technology*, *46*(6), 3060–3075. https://doi.org/10.1021/es2031505

30. Horn, DorothyA., Granek, E. F., & Steele, C. L. (2019). Effects of environmentally relevant concentrations of microplastic fibers on Pacific mole crab (*Emerita analoga*) mortality and reproduction. *Limnology and Oceanography Letters*. https://doi.org/10.1002/lol2.10137

31. Hu, D., Shen, M., Zhang, Y., Li, H., & Zeng, G. (2019). Microplastics and nanoplastics: Would they affect global biodiversity change? *Environmental Science and Pollution Research*, *26*(19), 19997–20002. https://doi.org/10.1007/s11356-019-05414-5

32. Hu, Y., Gong, M., Wang, J., & Bassi, A. (2019). Current research trends on microplastic pollution from wastewater systems: A critical review. *Reviews in Environmental Science and Bio/Technology*, *18*(2), 207–230. https://doi.org/10.1007/s11157-019-09498-w

33. Isobe, A., Kubo, K., Tamura, Y., Kako, S., Nakashima, E., & Fujii, N. (2014). Selective transport of microplastics and mesoplastics by drifting in coastal waters. *Marine Pollution Bulletin*, *89*(1–2), 324–330. https://doi.org/10.1016/j.marpolbul.2014.09.041

34. Kedzierski, M., Villain, J., Falcou-Préfol, M., Kerros, M. E., Henry, M., Pedrotti, M. L., & Bruzaud, S. (2019). Microplastics in Mediterranean Sea: A protocol to robustly assess contamination characteristics. *PLoS ONE*, *14*(2). https://doi.org/10.1371/journal.pone.0212088

35. Kettner, M. T., Oberbeckmann, S., Labrenz, M., & Grossart, H.-P. (2019). The Eukaryotic Life on Microplastics in Brackish Ecosystems. *Frontiers in Microbiology*, *10*. https://doi.org/10.3389/fmicb.2019.00538

36. Lares, M., Ncibi, M. C., Sillanpää, M., & Sillanpää, M. (2019). Intercomparison study on commonly used methods to determine microplastics in wastewater and sludge samples. *Environmental Science and Pollution Research*, *26*(12), 12109–12122. https://doi.org/10.1007/s11356-019-04584-6

37. Law, K. L. (2017). Plastics in the Marine Environment. *Annual Review of Marine Science*, *9*(1), 205–229. https://doi.org/10.1146/annurev-marine-010816-060409

38. Leslie, H. A., Brandsma, S. H., van Velzen, M. J. M., & Vethaak, A. D. (2017). Microplastics en route: Field measurements in the Dutch river delta and Amsterdam canals, wastewater treatment plants, North Sea sediments and biota. *Environment International*, *101*, 133–142. https://doi.org/10.1016/j.envint.2017.01.018

39. Li, J., Liu, H., & Paul Chen, J. (2018). Microplastics in freshwater systems: A review on occurrence, environmental effects, and methods for microplastics detection. *Water Research*, *137*, 362–374. https://doi.org/10.1016/j.watres.2017.12.056

40. Löder, M. G. J., Imhof, H. K., Ladehoff, M., Löschel, L. A., Lorenz, C., Mintenig, S., Piehl, S., Primpke, S., Schrank, I., Laforsch, C., & Gerdts, G. (2017). Enzymatic Purification of Microplastics in Environmental Samples. *Environmental Science & Technology*, *51*(24), 14283–14292. https://doi.org/10.1021/acs.est.7b03055

41. Löder, M., Imhof, H. K., Ladehoff, M., Löschel, L. A., Lorenz, C., Mintenig, S., Piehl, S., Primpke, S., Schrank, I., Laforsch, C., & Gerdts. (2017). *Suppprting Information—Enzymatic purification of microplastics in environmental samples*. 10.

42. Lusher, A. L., Welden, N. A., Sobral, P., & Cole, M. (2017). Sampling, isolating and identifying microplastics ingested by fish and invertebrates. *Analytical Methods*, *9*(9), 1346–1360. https://doi.org/10.1039/C6AY02415G

43. Maes, T., Jessop, R., Wellner, N., Haupt, K., & Mayes, A. G. (2017). A rapid-screening approach to detect and quantify microplastics based on fluorescent tagging with Nile Red. *Scientific Reports*, *7*(1). https://doi.org/10.1038/srep44501

44. Mason, S. A., Garneau, D., Sutton, R., Chu, Y., Ehmann, K., Barnes, J., Fink, P., Papazissimos, D., & Rogers, D. L. (2016). Microplastic pollution is widely detected in US municipal wastewater treatment plant effluent. *Environmental Pollution*, *218*, 1045–1054. https://doi.org/10.1016/j.envpol.2016.08.056

45. Mateos-Cárdenas, A., Scott, D. T., Seitmaganbetova, G., Frank N.A.M., van P., John, O., & Marcel A.K., J. (2019). Polyethylene microplastics adhere to Lemna minor (L.), yet have no effects on plant growth or feeding by Gammarus

duebeni (Lillj.). *Science of The Total Environment*, *689*, 413–421. https://doi.org/10.1016/j.scitotenv.2019.06.359

46. Mausra, J., Baker, J., Foster, G., & Arthur, C. (2015). Laboratory methods for the analysis of microplastics in the marine environment: Recommendations for quantifying synthetic particles in waters and sediments. *NOAA Technical Memorandum NOS-OR&R-48.*, 39.

47. McCormick, A., Hoellein, T. J., Mason, S. A., Schluep, J., & Kelly, J. J. (2014). Microplastic is an Abundant and Distinct Microbial Habitat in an Urban River. *Environmental Science & Technology*, *48*(20), 11863–11871. https://doi.org/10.1021/es503610r

48. Mendoza, L. M. R., & Jones, P. R. (2015). Characterisation of microplastics and toxic chemicals extracted from microplastic samples from the North Pacific Gyre. *Environmental Chemistry*. http://dx.doi.org/10.1071/EN14236

49. Michida, Y., Chavanich, S., Cabañas, A. C., Hagmann, P., Hinata, H., Isobe, A., Kershaw, P., Kozlovskii, N., Li, D., Martí, E., Mason, S. A., Mu, J., Saito, H., Shim, W. J., Syakti, A. D., Takada, H., Thompson, R., Tokai, T., Vasilenko, K., & Wang, J. (2019). Guidelines for Harmonizing Ocean Surface Microplastic Monitoring Methods. *Ministry of the Environment Japan*, 74.

50. Michielssen, M. R., Michielssen, E. R., Ni, J., & Duhaime, M. B. (2016). Fate of microplastics and other small anthropogenic litter (SAL) in wastewater treatment plants depends on unit processes employed. *Environmental Science: Water Research & Technology*, *2*(6), 1064–1073. https://doi.org/10.1039/C6EW00207B

51. Moore, C. J., Moore, S. L., Leecaster, M. K., & Weisberg, Stephen B. (2001). A Comparison of Plastic and Plankton in the North Pacific Central Gyre. *Marine Pollution Bulletin*, *42*(12), 1297–1300. https://doi.org/10.1016/S0025-326X(01)00114-X

52. NOAA: National Centers for Environmental Information (formerly the National Climatic Data Center). (2020, February 8). *Pacific Decadal Oscillation (PDO)* [Climate Monitoring Teleconnections]. Pacific Decadal Oscillation (PDO). https://www.ncdc.noaa.gov/teleconnections/pdo/

53. Northwest Fisheries Science Center. (2006). *Physical Oceanographic Considerations*. NOAA. https://www.nwfsc.noaa.gov/research/divisions/fe/estuarine/oeip/ja-physical-oceanographic-factors.cfm

54. Northwest Fisheries Science Center. (2013a). *Climate–Scale Physical Variability*. NOAA. https://www.nwfsc.noaa.gov/research/divisions/fe/estuarine/oeip/jb-climate-scale-phys-varia.cfm

55. Northwest Fisheries Science Center. (2013b). *Coastal Upwelling*. NOAA. https://www.nwfsc.noaa.gov/research/divisions/fe/estuarine/oeip/db-coastal-upwelling-index.cfm#CU-02

56. Northwest Fisheries Science Center. (2018). *Hydrography, Zooplankton, and Ichthyoplankton—Northwest Fisheries Science Center* [NOAA Research - Ecosystem Indicators]. Hydrography, Zooplankton, and Ichthyoplankton. https://www.nwfsc.noaa.gov/research/divisions/fe/estuarine/oeip/ka-hydrography-zoo-ichthyoplankton.cfm

57. Northwest Fisheries Science Center. (2019). *Annual summary of ocean ecosystem indicators for 2019*. NOAA. https://www.nwfsc.noaa.gov/research/divisions/fe/estuarine/oeip/b-latest-updates.cfm

58. OR&R Marine Debris Division. (2015, October 21). *Influence of Environmental Conditions on Contaminants Leaching From, and Sorbing To, Marine Microplastic Debris | OR&R's Marine Debris Program* [Text]. /research/influence-environmental-conditions-contaminants-leaching-and-sorbing-marine-microplastic, https://marinedebris.noaa.gov/research/influence-environmental-conditions-contaminants-leaching-and-sorbing-marine-microplastic

59. Piarulli, S., Scapinello, S., Comandini, P., Magnusson, K., Granberg, M., Wong, J. X. W., Sciutto, G., Prati, S., Mazzeo, R., Booth, A. M., & Airoldi, L. (2019). Microplastic in wild populations of the omnivorous crab Carcinus aestuarii: A review and a regional-scale test of extraction methods, including microfibres. *Environmental Pollution*, *251*, 117–127. https://doi.org/10.1016/j.envpol.2019.04.092

60. Portland State University. (2019, November 6). *Huge gaps in research on microplastics in North America* [Science News]. ScienceDaily. https://www.sciencedaily.com/releases/2019/11/191106154523.htm

61. Prata, Joana C., da Costa, J. P., Girão, A. V., Lopes, I., Duarte, A. C., & Rocha-Santos, T. (2019). Identifying a quick and efficient method of removing organic matter without damaging microplastic samples. *Science of The Total Environment*, *686*, 131–139. https://doi.org/10.1016/j.scitotenv.2019.05.456

62. Prata, Joana Correia, da Costa, J. P., Duarte, A. C., & Rocha-Santos, T. (2019). Methods for sampling and detection of microplastics in water and sediment: A critical review. *TrAC Trends in Analytical Chemistry*, *110*, 150–159. https://doi.org/10.1016/j.trac.2018.10.029

63. Profita, C., & Burns, J. (2019, July 30). Tiny Plastics Are A Big Problem: Microplastics Are Polluting Oregon's Rivers. In *OPB is examining the ways plastic is altering our relationship with the environment and what we can do about it*. OPB. https://www.opb.org/news/article/oregon-rivers-microplastic-pollution-investigation/

64. Puget Sound Institute. (2007). Climate and ocean processes. In *Encyclopedia of Puget Sound*. Retrieved from

https://www.eopugetsound.org/articles/climate-and-ocean-processes

65. Raju, S., Carbery, M., Kuttykattil, A., Senathirajah, K., Subashchandrabose, S. R., Evans, G., & Thavamani, P. (2018). Transport and fate of microplastics in wastewater treatment plants: Implications to environmental health. *Reviews in Environmental Science and Bio/Technology*, *17*(4), 637–653. https://doi.org/10.1007/s11157-018-9480-3

66. Rodrigues, M. O., Abrantes, N., Gonçalves, F. J. M., Nogueira, H., Marques, J. C., & Gonçalves, A. M. M. (2018). Spatial and temporal distribution of microplastics in water and sediments of a freshwater system (Antuã River, Portugal). *Science of The Total Environment*, *633*, 1549–1559. https://doi.org/10.1016/j.scitotenv.2018.03.233

67. Ryan, P. G. (2015). A Brief History of Marine Litter Research. In M. Bergmann, L. Gutow, & M. Klages (Eds.), *Marine Anthropogenic Litter* (pp. 1–25). Springer International Publishing. https://doi.org/10.1007/978-3-319-16510-3_1

68. Scherer, C., Brennholt, N., Reifferscheid, G., & Wagner, M. (2017). Feeding type and development drive the ingestion of microplastics by freshwater invertebrates. *Scientific Reports*, *7*(1), 1–9. https://doi.org/10.1038/s41598-017-17191-7

69. Shim, W. J., Hong, S. H., & Eo, S. E. (2017). Identification methods in microplastic analysis: A review. *Analytical Methods*, *9*(9), 1384–1391. https://doi.org/10.1039/C6AY02558G

70. Shim, W. J., Song, Y. K., Hong, S. H., & Jang, M. (2016). Identification and quantification of microplastics using Nile Red staining. *Marine Pollution Bulletin*, *113*(1), 469–476. https://doi.org/10.1016/j.marpolbul.2016.10.049

71. Simmerman, C. B., & Coleman Wasik, J. K. (2019). The effect of urban point source contamination on microplastic levels in water and organisms in a cold-water stream. *Limnology and Oceanography Letters*. https://doi.org/10.1002/lol2.10138

72. Stanton, T., Johnson, M., Nathanail, P., Gomes, R. L., Needham, T., & Burson, A. (2019). Exploring the Efficacy of Nile Red in Microplastic Quantification: A Costaining Approach. *Environmental Science & Technology Letters*, *6*(10), 606–611. https://doi.org/10.1021/acs.estlett.9b00499

73. Sun, J., Dai, X., Wang, Q., van Loosdrecht, M. C. M., & Ni, B.-J. (2019). Microplastics in wastewater treatment plants: Detection, occurrence and removal. *Water Research*, *152*, 21–37. https://doi.org/10.1016/j.watres.2018.12.050

74. Tamminga, M., Hengstmann, E., & Fischer, E. K. (2017). Nile Red Staining as a Subsidiary Method for Microplastic Quantifica-tion: A Comparison of Three Solvents and Factors Influencing Application Reliability. *SDRP Journal of Earth Sciences & Environmental Studies*, *2*(2). https://doi.org/10.15436/JESES.2.2.1

75. Thermo Fisher Scientific Inc. (2014). *A guide to laboratory filtration*. Fisher Scientific - Distributer GE Healthcare. http://static.fishersci.com/cmsassets/downloads/segment/Scientific/pdf/GE/whatman-filtration-ge-healthcare-selection-guide.pdf

76. Thiele, C. J., Hudson, M. D., & Russell, A. E. (2019). Evaluation of existing methods to extract microplastics from bivalve tissue: Adapted KOH digestion protocol improves filtration at single-digit pore size. *Marine Pollution Bulletin*, *142*, 384–393. https://doi.org/10.1016/j.marpolbul.2019.03.003

77. Turner, A., & Holmes, L. A. (2015). Adsorption of trace metals by microplastic pellets in fresh water. *Environmental Chemistry*, *12*(5), 600. https://doi.org/10.1071/EN14143

78. UCLA STATISTICAL CONSULTING GROUP, & Institute for Digital Research & Education. (2019). *Introduction to Linear Mixed Models* [Educational]. Introduction to Linear Mixed Models. https://stats.idre.ucla.edu/other/mult-pkg/introduction-to-linear-mixed-models/

79. Valine, A. (2019). *Nile Red Microplastic Validation: Enhancing the Study of Microplastics in Oregon's River Water* [Portland State University]. https://doi.org/10.15760/honors.794

80. Wardrop, P., Shimeta, J., Nugegoda, D., Morrison, P. D., Miranda, A., Tang, M., & Clarke, B. O. (2016). Chemical Pollutants Sorbed to Ingested Microbeads from Personal Care Products Accumulate in Fish. *Environmental Science & Technology*, *50*(7), 4037–4044. https://doi.org/10.1021/acs.est.5b06280

81. Wiggin, K. J., & Holland, E. B. (2019). Validation and application of cost and time effective methods for the detection of 3–500 µm sized microplastics in the urban marine and estuarine environments surrounding Long Beach, California. *Marine Pollution Bulletin*, *143*, 152–162. https://doi.org/10.1016/j.marpolbul.2019.03.060

82. Windsor, F. M., Tilley, R. M., Tyler, C. R., & Ormerod, S. J. (2019). Microplastic ingestion by riverine macroinvertebrates. *Science of The Total Environment*, *646*, 68–74. https://doi.org/10.1016/j.scitotenv.2018.07.271

83. Worm, B., Lotze, H. K., Jubinville, I., Wilcox, C., & Jambeck, J. (2017). Plastic as a Persistent Marine Pollutant. *Annual Review of Environment and Resources*, *42*(1), 1–26. https://doi.org/10.1146/annurev-environ-102016-060700

84. Wu, C., Zhang, K., & Xiong, X. (2018). Microplastic Pollution in Inland Waters Focusing on Asia. In M. Wagner & S. Lambert (Eds.), *Freshwater Microplastics: Emerging Environmental Contaminants?* (pp. 85–99). Springer International Publishing. https://doi.org/10.1007/978-3-319-61615-5_5

85. YSI Inc. / Xylem Inc. (n.d.). *The Basics of Chlorophyll Measurement*. 3.

Appendix

A ▸ *Detailed Conceptual Framework - Graphical Methods*

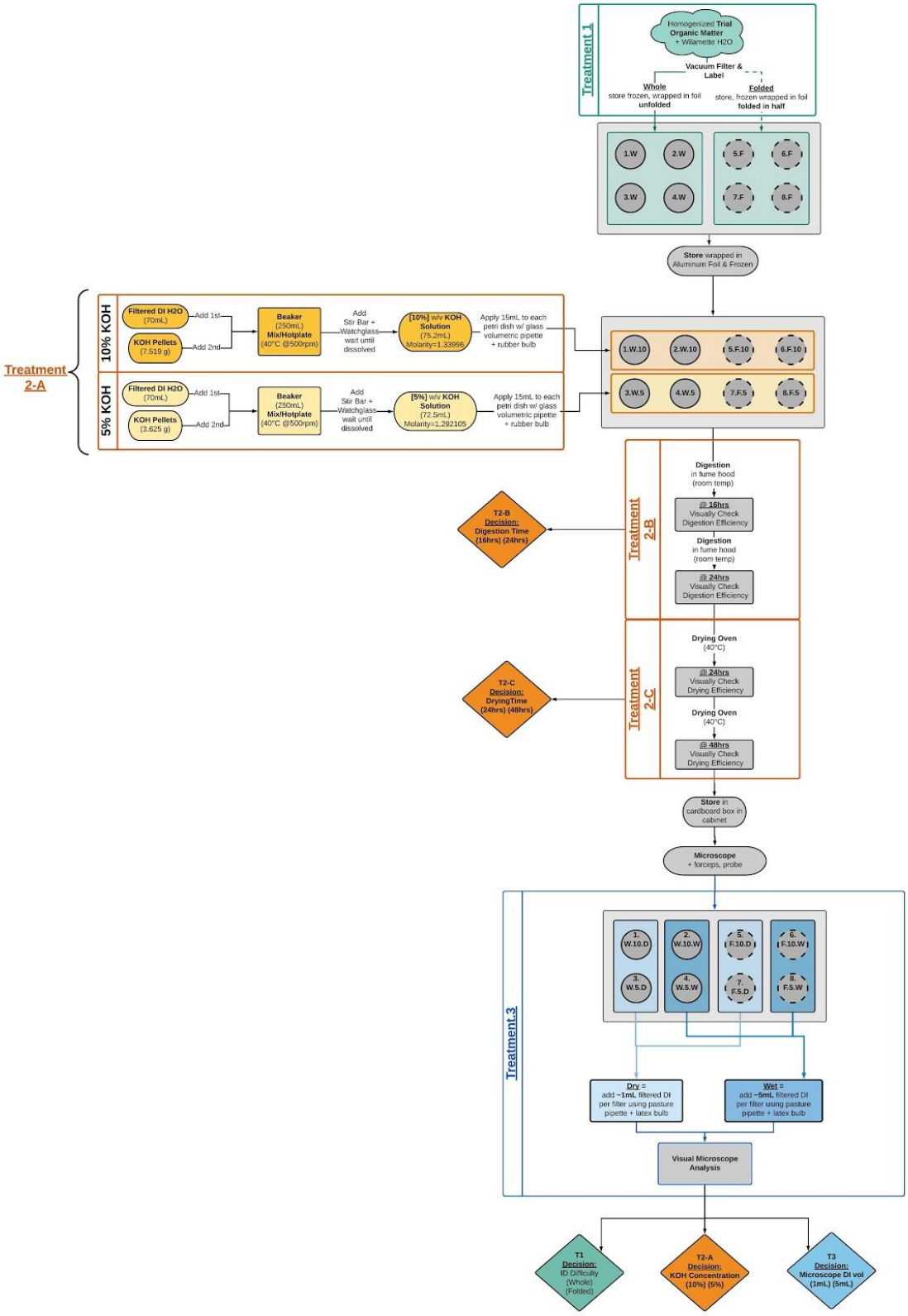

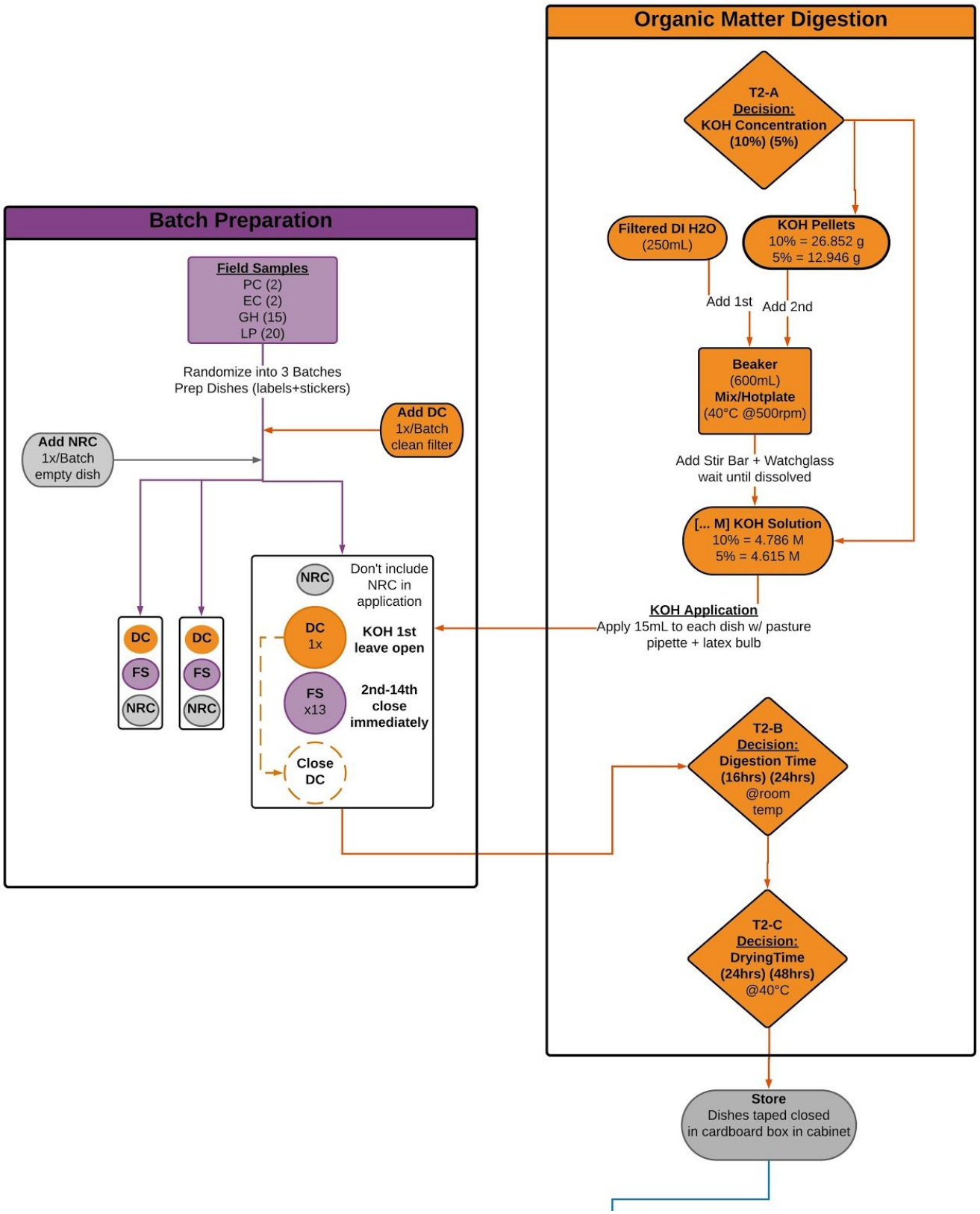
Organic Matter Digestion
T2-A
Decision:
KOH Concentration
(10%) (5%)
Filtered DI H2O
(250mL)
KOH Pellets
10% = 26.852 g
5% = 12.946 g
Add 1st
Add 2nd
Beaker
(600mL)
Mix/Hotplate
(40°C @500rpm)
Add Stir Bar + Watchglass
wait until dissolved
[... M] KOH Solution
10% = 4.786 M
5% = 4.615 M
KOH Application
Apply 15mL to each dish w/ pasture
pipette + latex bulb
Batch Preparation
Field Samples
PC (2)
EC (2)
GH (15)
LP (20)
Randomize into 3 Batches
Prep Dishes (labels+stickers)
Add DC
1x/Batch
clean filter
Add NRC
1x/Batch
empty dish
DC
FS
NRC
DC
FS
NRC
NRC
Don't include
NRC in
application
DC
1x
KOH 1st
leave open
FS
x13
2nd-14th
close
immediately
Close
DC
T2-B
Decision:
Digestion Time
(16hrs) (24hrs)
@room
temp
T2-C
Decision:
DryingTime
(24hrs) (48hrs)
@40°C
Store
Dishes taped closed
in cardboard box in cabinet

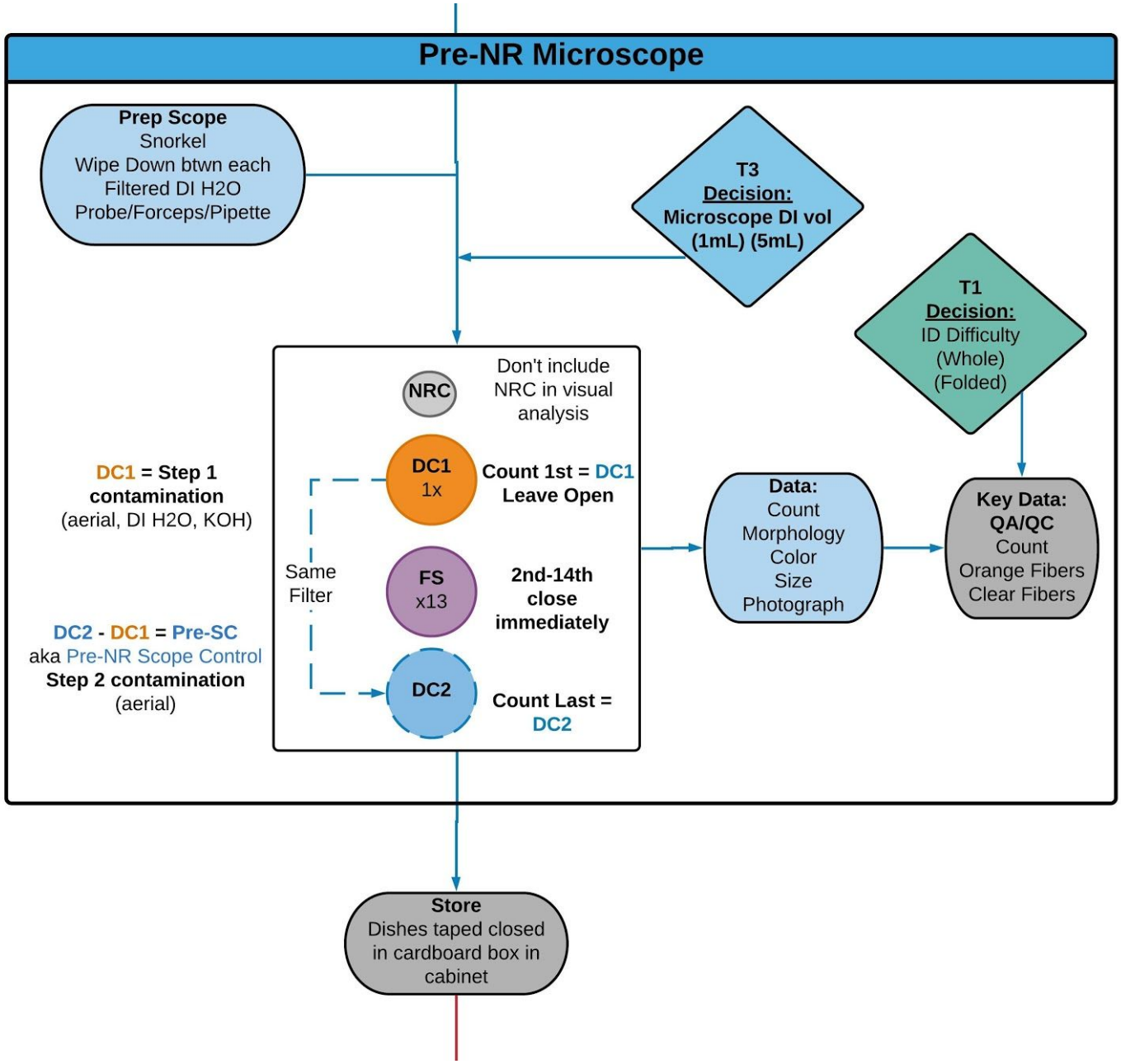
Pre-NR Microscope
Prep Scope
Snorkel
Wipe Down btwn each
Filtered DI H2O
Probe/Forceps/Pipette
T3
Decision:
Microscope DI vol
(1mL) (5mL)
T1
Decision:
ID Difficulty
(Whole)
(Folded)
NRC
Don't include NRC in visual analysis
DC1
1x
Count 1st = DC1
Leave Open
Same Filter
FS
x13
2nd-14th close immediately
DC2
Count Last = DC2
DC1 = Step 1 contamination
(aerial, DI H2O, KOH)
DC2 - DC1 = Pre-SC
aka Pre-NR Scope Control
Step 2 contamination
(aerial)
Data:
Count
Morphology
Color
Size
Photograph
Key Data:
QA/QC
Count
Orange Fibers
Clear Fibers
Store
Dishes taped closed in cardboard box in cabinet

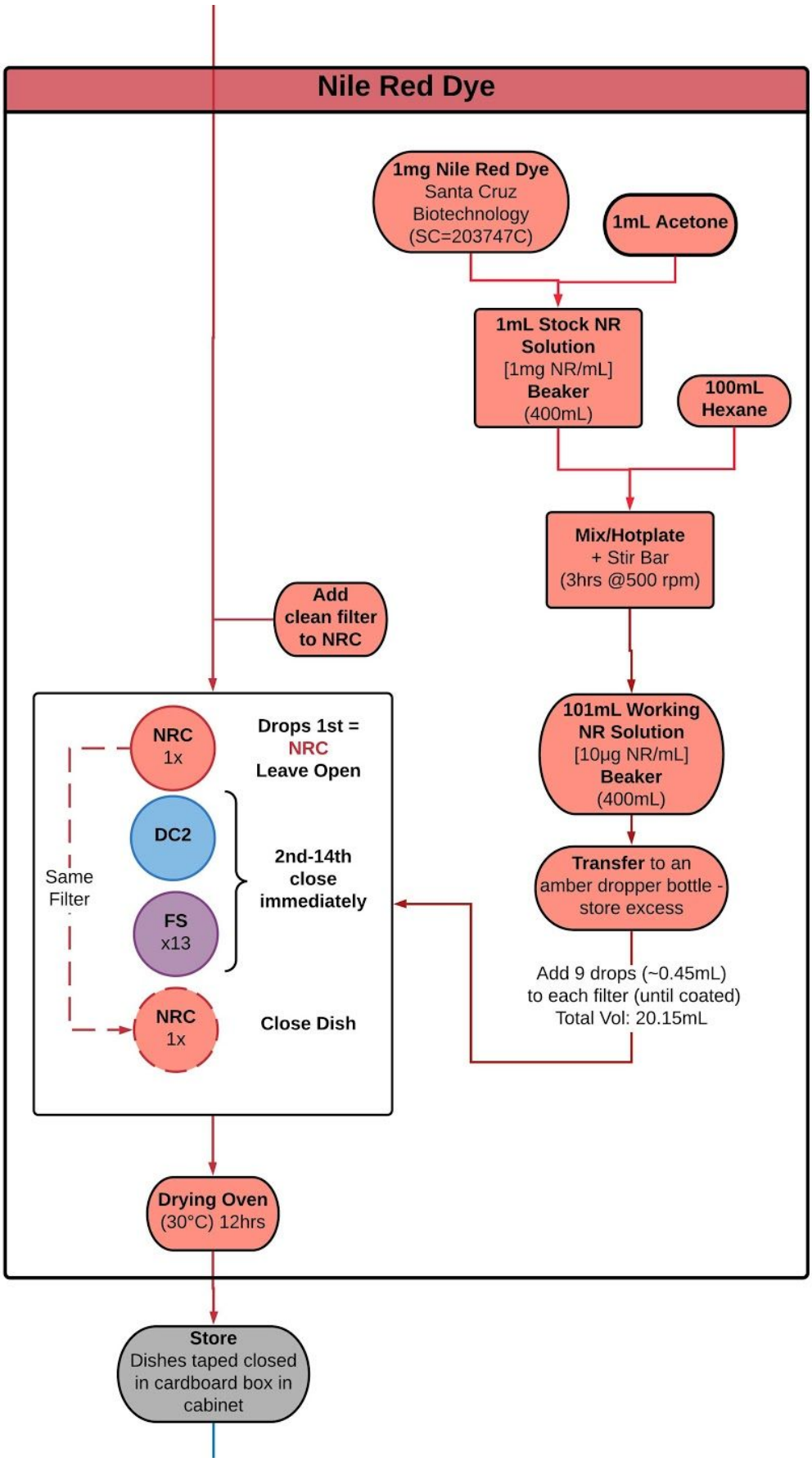
Nile Red Dye
1mg Nile Red Dye
Santa Cruz
Biotechnology
(SC=203747C)
1mL Acetone
1mL Stock NR
Solution
[1mg NR/mL]
Beaker
(400mL)
100mL
Hexane
Mix/Hotplate
+ Stir Bar
(3hrs @500 rpm)
Add
clean filter
to NRC
101mL Working
NR Solution
[10µg NR/mL]
Beaker
(400mL)
Transfer to an
amber dropper bottle -
store excess
Add 9 drops (~0.45mL)
to each filter (until coated)
Total Vol: 20.15mL
NRC
1x
Drops 1st =
NRC
Leave Open
DC2
2nd-14th
close
immediately
Same
Filter
FS
x13
NRC
1x
Close Dish
Drying Oven
(30°C) 12hrs
Store
Dishes taped closed
in cardboard box in
cabinet

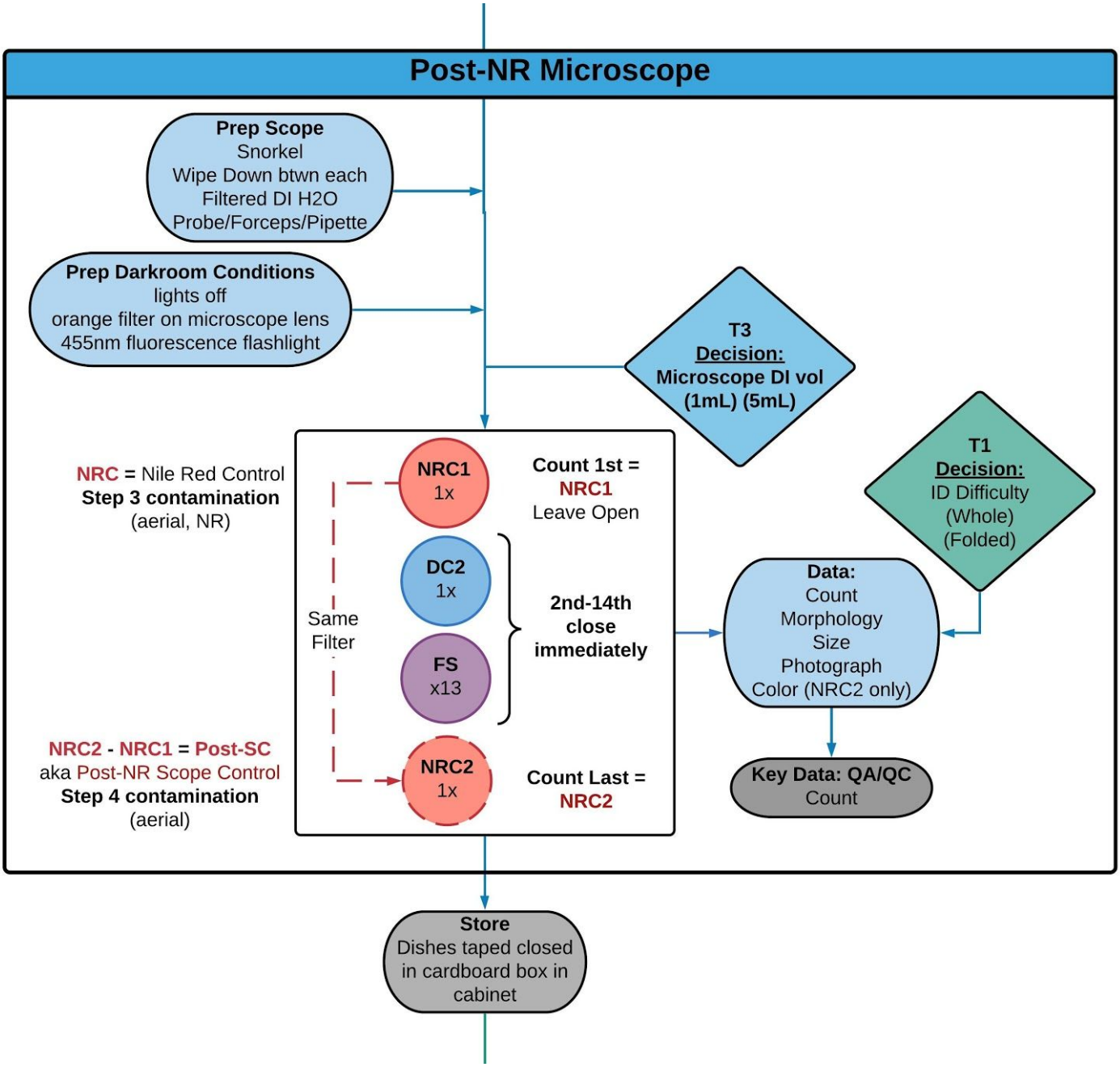
Post-NR Microscope
Prep Scope
Snorkel
Wipe Down btwn each
Filtered DI H2O
Probe/Forceps/Pipette
Prep Darkroom Conditions
lights off
orange filter on microscope lens
455nm fluorescence flashlight
T3
Decision:
Microscope DI vol
(1mL) (5mL)
T1
Decision:
ID Difficulty
(Whole)
(Folded)
NRC = Nile Red Control
Step 3 contamination
(aerial, NR)
NRC1
1x
Count 1st =
NRC1
Leave Open
DC2
1x
FS
x13
2nd-14th
close
immediately
Same
Filter
Data:
Count
Morphology
Size
Photograph
Color (NRC2 only)
NRC2 - NRC1 = Post-SC
aka Post-NR Scope Control
Step 4 contamination
(aerial)
NRC2
1x
Count Last =
NRC2
Key Data: QA/QC
Count
Store
Dishes taped closed
in cardboard box in
cabinet

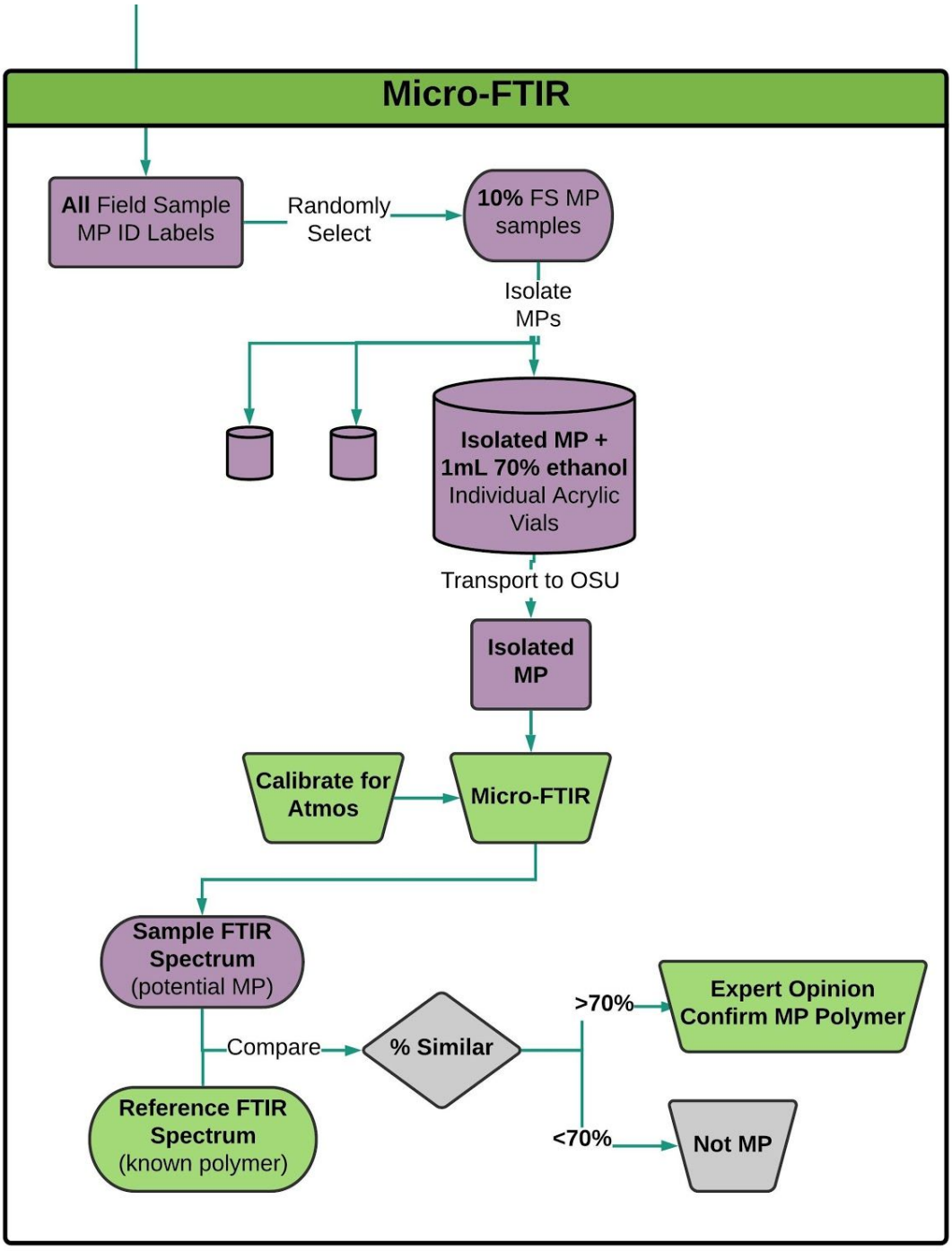
Micro-FTIR
All Field Sample MP ID Labels
Randomly Select
10% FS MP samples
Isolate MPs
Isolated MP + 1mL 70% ethanol Individual Acrylic Vials
Transport to OSU
Isolated MP
Calibrate for Atmos
Micro-FTIR
Sample FTIR Spectrum (potential MP)
Compare
% Similar
>70%
Expert Opinion Confirm MP Polymer
<70%
Not MP
Reference FTIR Spectrum (known polymer)